NASA TECHNICAL NOTE

NASA TN D-1952

NASA TN D-1952

MEASURED VARIATION IN THE TRANSFER FUNCTION OF A HUMAN PILOT IN SINGLE-AXIS TASKS

by James J. Adams and Hugh P. Bergeron;
Langley Research Center,
Langley Station, Hampton, Va.

NATIONAL AERONAUTICS AND SPACE ADMINISTRATION • WASHINGTON, D.C. • OCTOBER 1963

TECHNICAL NOTE D-1952

MEASURED VARIATION IN THE TRANSFER FUNCTION OF A HUMAN PILOT IN SINGLE-AXIS TASKS

By James J. Adams and Hugh P. Bergeron

Langley Research Center
Langley Station, Hampton, Va.

NATIONAL AERONAUTICS AND SPACE ADMINISTRATION

NATIONAL AERONAUTICS AND SPACE ADMINISTRATION

TECHNICAL NOTE D-1952

MEASURED VARIATION IN THE TRANSFER FUNCTION OF A HUMAN PILOT IN SINGLE-AXIS TASKS

By James J. Adams and Hugh P. Bergeron

SUMMARY

Measurements of the variations in the transfer function of a human pilot, relating visual stimuli to stick controller output, in a single-degree-of-freedom fixed-base simulator have been made by using an automatic model matching technique. Variations in subjects, controlled dynamics (from simple amplifiers to a double integration), display sensitivity, control sensitivity, and type of task (from compensatory tracking to pursuit tracking) were included in the tests.

The results show that the pilot changes his transfer function whenever any element in the control loop is changed. Whereas wide variations in the transfer functions were measured, variations in the closed-loop characteristics were much more restricted.

INTRODUCTION

In the experiments reported in this paper an attempt has been made to measure quantitatively what a human pilot does when operating in a closed-loop single-degree-of-freedom attitude-control system. The quantity measured is a transfer function with three variable gains which relate the visual stimuli provided to the pilot to his stick controller deflection. This transfer function is mechanized with analog-computer equipment. The variable gains in the analog pilot are adjusted so that the square of the difference between the output of the human pilot and the output of the analog pilot is minimized. The method used to achieve the necessary adjustment of the analog pilot gains is similar to that used in an advanced adaptive autopilot and is described in reference 1.

The experiment is an extension of several other studies reported in references 2 to 6, which also determined transfer functions of human pilots by matching frequency-response plots with an analytical expression. The frequency-response data were usually obtained by making a power-spectral-density analysis of the recorded time histories of the tests. This type of analysis is very lengthy and complicated. In contrast, the method of analysis used in the present tests provides the desired results during the experiment. The simplicity of the analysis plus the flexibility afforded by the simulator used in conducting the tests allowed wide variations in several of the elements in the system to be

studied. The simulated controlled dynamics were varied from a simple amplification of the pilot's stick output to a second integral of the pilot's stick output. The sensitivity of the stick controller and the sensitivity of the display were also varied. Six experienced test pilots and two engineers were used as subjects. The measured transfer function gains together with the derived characteristics of the complete system (pilot plus dynamics) are presented in this paper.

The transfer functions determined in these tests might be used in simple, linear analytical design studies. Further work will be required before they can be applied to more practical multi-axes, nonlinear studies. The method for making the measurements might be used to evaluate system design concepts.

SYMBOLS

D	disturbance, volts
I	generalized input (either D or ϵ as noted), volts
K,α	general gains
K_1,K_2	particular computer gains
s	Laplace transform, sec^{-1}
x	difference between pilot output and analog pilot output
δ	analog pilot output, volts
δ',δ''	output of analog pilot at intermediate points, volts
ϵ	displayed error, volts
ζ	damping ratio
θ	system output, volts
τ	lag break point frequency, radians/sec
ω	undamped natural frequency, radians/sec

APPARATUS

Shown in figure 1 is a block diagram of the elements used in the experiments, and a photograph of the simulator and computer is shown in figure 2. The control loop consists of the following elements.

An oscilloscope is used to present the visual display of the problem to the pilot. A horizontal line presented on the oscilloscope moved up and down approximately 2 inches. The oscilloscope sensitivity was set, normally, so that the uncontrolled disturbance used in these tests would drive the horizontal line to the full 2-inch deflection. The pilot, by exercising control, kept the indicated deflection to lower values.

The pilot exercised control with a centrally located, lightweight control stick which moved forward and backward. This stick was supported by ball bearings so as to be as nearly frictionless as possible. A spring was also included which provided a force that was linearly proportional with deflection and provided a 2.5-pound force at full deflection. Full deflection was approximately ±3 inches at the top of the stick. A linear potentiometer was attached to the stick to provide the required electrical signal. The maximum output of this potentiometer was ±10 volts.

The simulated dynamics were obtained with an analog computer and were very simple examples of different order systems. The transfer functions relating output to input of the simulated dynamics are 1, $\frac{1}{s+1}$, $\frac{10}{s^2+3s+10}$, $\frac{2}{s}$ or $\frac{4}{s}$, $\frac{10}{s(s+1)}$, and $\frac{10}{s^2}$. In addition, in repeated tests with pilot E, the following two dynamics were also included: $\frac{10}{s(s+2.5)}$ and $\frac{10}{s(s^2+3s+10)}$. The equipment required for these dynamics consisted of two amplifier-integrators and, in some cases, gain-setting potentiometers and sign-changing amplifiers. The variation in dynamics was achieved by changing one or both of the amplifier-integrators from amplifiers to integrators and adding one or two feedback loops. The dynamics will be referred to as though the display represented the angular position of the vehicle. Thus, the first three will be referred to as attitude dynamics; that is, the steady-state output of the dynamics is proportional to stick deflection. The remaining ones will be called rate and acceleration dynamics.

A disturbance signal was inserted into the control loop to provide a certain work load for the pilot. This disturbance was obtained by filtering the output of a Gaussian noise generator. The filter consisted of two first-order lags with break frequencies that were usually located at 1 radian per second for the attitude dynamics and 0.5 radian per second for the rate and acceleration dynamics. The few exceptions to these settings are noted in the data. Also, in two series of tests, a cam-generated disturbance was used. This disturbance contained 12 frequencies with approximately equal amplitude. The highest frequency was approximately 2 radians per second.

The problem was presented as a compensatory tracking task. The disturbance signal and the output of the dynamics were summed and then presented on the display. The pilot's task was to keep the indicated signal alined with a fixed reference line on the display. In addition, some tests were made in which the disturbance was applied to one line of a dual beam presentation and the pilot's effort displayed on a second line. The pilot was required to keep the two lines together. These tests are referred to as pursuit tracking tests. Note that in the compensatory tracking task, the disturbance as used in these tests corresponds

to the output of the uncontrolled vehicle subject to some unspecified external force and not to the external force itself. In the case of the pursuit tracking task, the disturbance corresponds to the movement of the target being tracked.

The computer was also used to form the analog pilot which was matched to the human pilot and to make the computation necessary for adjusting the variable gains in the analog pilot. These variable gains were mechanized with servo multipliers. A brief derivation of the gain-changing method is presented in appendix A and is also given in reference 1. The method is derived from an adaptive autopilot scheme presented in reference 7. There is one difference in lead-time constant-gain adjustment from that used in reference 1; that is, the integrator included in the lead-time constant-gain filter was omitted in the present study. (See K_2 block in computer diagram and fig. 3 in ref. 1.)

The analytic form of the computer analog pilot is

$$\frac{\delta}{I} = \frac{K_1\tau\left(1 + \frac{K_2}{\tau}s\right)}{(\tau + s)^2} \tag{1}$$

This form was not changed in the experiments; only the gains, K_1, τ, and K_2, were variable. The results must be viewed with this in mind. This particular form was selected because previous investigations have shown that a transfer function of this general form will provide a good fit to the pilot. There are, however, two alterations from some of the previous investigations. A time-delay term, generally expressed as e^{-Ks}, which has been included by previous investigators was omitted in the present tests. Also, in previous investigations, the lag terms (the two first-order factors in the denominator) have been assumed to be different from each other, whereas in the present tests they were assumed to be the same. The data of reference 2 show that the best fit was achieved with the form given in equation (1), and it is for this reason that this particular form was chosen for study.

The assumption of this form of transfer function implies that the pilot uses the sum of the amplitude of the input and the rate of change of the input with some lag to determine the amplitude of his stick displacement. This lag is expressed as two equal first-order lags.

In many of the previous investigations the transfer function which was determined related pilot output to displayed error. In the present investigation this is true only in the cases in which rate and acceleration dynamics are used. In the cases in which attitude dynamics are used, the function determined relates pilot output to disturbance; that is, the disturbance signal is used as the input to the analog pilot in the case of attitude dynamics and the displayed error (the sum of the disturbance and the output of the dynamics) is used as the input to the analog pilot in the cases of the rate and acceleration dynamics. The reasons for this method of analysis are discussed in reference 1. It will be clearly indicated in the data which quantity is used as the input.

When numerical results are given for the transfer function in the tables, they are given in this form

$$\frac{\delta}{I} = \frac{\frac{K_1}{\tau}\left(1 + \frac{K_2}{\tau}s\right)}{\left(1 + \frac{1}{\tau}s\right)^2} \tag{2}$$

where $\frac{K_1}{\tau}$ is the static gain, which has the units volts per volt; $\frac{K_2}{\tau}$ is the lead time constant, which has the units seconds; and $\frac{1}{\tau}$ is the lag time constant, which has the units seconds. The data are presented in this form because it is the one generally used by system designers. For reasons of computer compatibility it was necessary to mechanize the analog pilot in the manner given in equation (1).

TESTS AND ANALYSIS

Six experienced NASA test pilots and two research engineers were used as subjects in these tests. The pilots all had flying experience in a wide variety of airplane types ranging from jet fighters to helicopters, and, in addition, pilots A to D had considerable experience in operating simulators of both airplanes and space vehicles. The engineers had no more than ordinary control experience, but, of course, did have a thorough analytical knowledge of the control problems used in the tests. The pilots are listed from A to F in descending order of their age and experience, pilot A being 47 years old with 16 years experience with NASA, and pilot F being 30 years old and just out of military service. In the tests the pilots were asked to use the control in whatever manner they felt would keep the indicator as close to the reference mark as possible. The subjects were given a warm-up run which lasted as long as they wished, but which did not usually exceed 2 minutes. A 3-minute test run was then taken. This procedure was followed for each of the dynamics. The tests were always given in the same order, with the attitude dynamics first and the acceleration dynamics last, except in the repeat tests with pilot E when the order was reversed.

The numerators of the simulated dynamics were adjusted in each case so that the stick motions used in each test were in a comfortable range. That is, it was adjusted so that the control was not judged to be too sensitive, and so that full deflection was not required in controlling the disturbance. The following table is presented to illustrate the relative control power that was simulated in the tests. The table gives the maximum attitude, velocity, and acceleration available in each test if the stick was moved in a step to full deflection. Once again it is assumed that the indicator presents attitude.

Dynamics	Acceleration, volts/sec^2	Velocity, volts/sec	Attitude, volts
1	∞	∞	10
$\frac{1}{s+1}$	∞	10	10
$\frac{10}{s^2+3s+10}$	100	17	10
$\frac{2}{s}$	∞	20	∞
$\frac{10}{s(s+1)}$	100	100	∞
$\frac{10}{s^2}$	100	∞	∞

Note that the values of infinite acceleration given in this table represent pulses that occur at zero time, whereas the values of infinite attitude represent an ever increasing angle with time.

The nominal oscilloscope sensitivity was 5 volts per inch. If the display is considered as a simulated instrument display, it would represent a rather large instrument. Additional tests were made in which the oscilloscope sensitivity was set so as to give smaller indicator deflections (50 volts per inch) in one case, and larger deflection in another (1.25 volts per inch). In this latter case the pilot had a tendency to drive the indicator off scale. These tests were made with $\frac{10}{s(s+1)}$ dynamics.

Other tests were made in which the control power was reduced. These tests were all made with $\frac{K}{s(s+1)}$ dynamics. The numerator was reduced from the nominal value of 10 to 5, 2, and 1.

For each test, the analog pilot gains, as they appear in equation (1), were obtained. The corresponding transfer function, as given in equation (2), was then determined. For additional information, the closed-loop transfer functions (pilot plus dynamics) relating system output θ to the disturbance D were determined, and the characteristic roots calculated. Example derivations of the closed-loop transfer functions are given in appendix B. Frequency-response plots of the closed-loop systems for tests made with pilot E were also made.

RESULTS AND DISCUSSION

General

Sample test runs for all the dynamics used are shown in figures 3 to 8. The subject in these tests is pilot E. The disturbance, the displayed error, the pilot's output, the analog pilot's output, and the difference between the latter two are shown in the first part of the figures, and adjustment of the three gains is shown in the second part of the figures. It can be seen that the adjustment of the gains is rapid and reaches a fairly steady value with only small variations in less than 30 seconds. The difference between the analog pilot and the human pilot reaches a fairly uniform minimum after the adjustment is completed. To illustrate the match between pilot and analog pilot, two samples with an expanded time scale are shown in figures 9 and 10. It can be seen that the analog pilot follows the low frequencies of the pilot both in time and amplitude but does not contain some of the high frequencies that appear in the pilot's output.

Variation With Dynamics

Data taken from all the tests with all the subjects are listed in table I. The tables list dynamics, the noise break frequency of the disturbance, the measured gains, the transfer function, and the characteristics of the closed-loop system. A sample run, using the $\frac{10}{s(s + 1)}$ dynamics, for each of the subjects is shown in figures 11 to 17.

It can be seen that all the gains, K_1, τ, and K_2, vary with change in dynamics, and the variations are different with each subject. Nevertheless, some general statements can be made about these variations. With the attitude dynamics in the case of the change from dynamics of 1 to the first-order lag $\frac{1}{1 + s}$ the lead time constant is increased to approximately 1, the lag time constant increases slightly, and the static gain remains nearly the same at a value of approximately 1. The pilot, therefore, can effectively be considered to be canceling the lag introduced into the dynamics and thus maintaining the overall dynamics of the closed-loop system unchanged. The further change to the oscillatory dynamics $\frac{10}{s^2 + 3s + 10}$ results in a noticeable reduction in the static gain. It is logical to assume that if a single step disturbance were presented to the pilot in this case, he would operate in a manner that would indicate a static gain of 1; that is, he would reduce the error to zero. It appears that the measured static gains of less than 1 results from the type of disturbance used in these tests. A similar result was noted in tests reported in reference 6.

With the attitude dynamics, where the function δ/D was measured, the closed-loop characteristic expression is exactly equal to the product of these factors - the denominator of the controlled dynamics and the denominator of the pilot's transfer function. Since it is therefore obvious what the closed-loop characteristics are, they are not listed in the tables.

With the dynamics that included integration, all subjects displayed a decrease in lag time constants in going from a rate system $\frac{2}{s}$ to an acceleration system $\frac{10}{s^2}$, the pilot's lag with the system $\frac{10}{s(s+1)}$ being intermediate between the latter two. All subjects displayed some lead, but there were large variations in the amount of lead measured, particularly with the rate dynamics, and also large variations in the measured static gains. However, all the subjects did show a consistent variation in the closed-loop frequency and damping characteristics with a change in dynamics. Both frequency and damping ratio decrease in going from a rate system to an acceleration system. With the rate system most of the subjects had a frequency of approximately 3.5 radians per second, pilots A and B having higher than this value. The damping ratio was approximately 0.7 in most cases. With the acceleration dynamics the closed-loop frequencies dropped to approximately 2.5 radians per second, and the damping ratios dropped to approximately 0.2.

Frequency-response plots for the closed-loop systems with pilot E as the operator, using the data listed in table II(b) and table II(c), are shown in figures 18 and 19. These figures illustrate the fact that, although the characteristic frequency is reduced in going from a rate system to an acceleration system, the resonance peaks that appear in the frequency-response plots are located at the same or even higher frequencies.

The reason for the decrease in lag time constants in going from a rate to an acceleration system might be explained as follows. With the well-behaved easy-to-handle rate system, the pilot can achieve what he considers to be a satisfactory control with a large lag. He therefore takes advantage of this allowance. With the more difficult acceleration dynamics, the pilot must reduce his own lag to achieve satisfactory control, and he does. Since the closed-loop characteristics generally show a decrease in period or damping or both when going from a rate to an acceleration system, it appears that the pilot is not able to reduce his lag enough to maintain the same level of control.

In an attempt to answer in greater detail why the pilot changes gains when the dynamics are changed, the gains that were measured with the rate system and the acceleration system were applied to the $\frac{10}{s(s+1)}$ system and the closed-loop characteristics determined. When the rate system gains were used, the damping of the closed-loop system underwent a large decrease, usually to a negative value, or the real roots were reduced, or both, when compared with the results obtained when using the gains measured with the $\frac{10}{s(s+1)}$ system. The frequency showed only small, random variations. It appears therefore that both the system damping and real roots are given consideration by the pilot in adjusting his gains, or technique, to achieve the characteristics which he desires. When the acceleration system gains were used, there was very little change. The changes that did occur were an increase in damping and an increase in the lowest real root. This result indicates that the pilot is capable of better control with the $\frac{10}{s(s+1)}$ system than he actually displays, but in these tests he did not exercise this better control.

Variation With Subjects

The highest static gains, high lead time constants, and the lowest lag time constants were measured with pilot A. Correspondingly, the characteristics of the closed-loop system, using the transfer function for pilot A, show the highest frequency, damping ratio, and real roots for any given dynamics. A review of the error records also shows that pilot A achieved the tightest control. In contrast, the damping ratios and real roots obtained with the engineers were the lowest determined in the tests.

Variations From Day to Day

Pilot E was retested on several different days. Results of these tests are given in table II, and sample runs with $\frac{10}{s(s + 1)}$ dynamics are shown in figures 20 to 21. The time histories show that there are variations in the manner in which the pilot operated his stick on different days. There were corresponding variations in the measured analog pilot gains and in the transfer function. A comparison made with the $\frac{10}{s(s + 1)}$ dynamics show that the closed-loop frequency characteristic varied from 2.5 to 4.4 radians per second, the damping ratio varies from 0.3 to 0.5, and the lowest real root varies from 0.5 to 4.0. This spread in data indicates that more testing on day-to-day variations should be conducted to establish better the limits on these variations.

Root-mean-square error values, which were not measured in the initial tests, were taken during these retests. The values of root-mean-square error given for the third-day tests (table II(b)) correspond to the error time histories shown in figures 3 to 8, the sample runs. The root-mean-square value of the disturbance for each run was not measured, but a sample value for the disturbance is 2.7 volts. Except for the $\frac{10}{s^2}$ case on the second test, the pilot always reduced the root-mean-square error below the value for the disturbance alone. The $\frac{10}{s^2}$ test on the second day was a short run and should not be given equal weight with the other tests. The root-mean-square error values also confirm the fact that the acceleration dynamics were more difficult to control than the rate dynamics, since lower values were always obtained with the rate dynamics.

Variations With Display Sensitivity

Pilot E was also used in tests in which the oscilloscope sensitivity was varied. Tabulated results of these tests are presented in table III, and sample time histories are shown in figures 22 and 23. Decreasing the sensitivity (50 volts per inch) from the nominal value (5 volts per inch) caused a large reduction in the static gain of the transfer function. The closed-loop system oscillatory characteristics show a reduction in frequency and an increase in damping ratio, while the real roots remain unchanged as compared with the results obtained with the nominal sensitivity. The root-mean-square error was increased.

Note that this root-mean-square error refers to the error signal in volts and not to the displacement in inches of the signal display. The sensitivity was also increased (1.5 volts per inch) to the point where the pilot could just keep the indicator within the display limits. With this sensitivity the static gain was increased, the closed-loop system oscillatory characteristics showed an increase in frequency and a decrease in damping ratio. The root-mean-square error remains the same as with the nominal sensitivity setting.

Variations With Control Sensitivity

Tabulated data of results obtained with reduced control sensitivity with $\frac{K}{s(s+1)}$ dynamics are presented in table IV, and sample time histories are shown in figures 24 and 25. When the stick sensitivity was reduced from 10 to 5, the static gain increased with an inverse proportional relation so that the closed-loop characteristics were not changed. Further reduction in the control sensitivity resulted in a further increase in pilot static gain but this increase was less than exactly inversely proportional to the sensitivity change and therefore the closed-loop system oscillatory characteristics showed a decrease in frequency. The lowest real root increased, and the highest real root decreased as the sensitivity was reduced. The root-mean-square error was not affected by the change. It should be noted that with the lowest sensitivity used the pilot frequently moved the stick to full deflection.

Other Variations

In some scattered tests, the variation was in the disturbance break frequency. In table I are listed some instances in which the noise break frequency was changed from 1 radian per second to 0.5 radian per second with the rate dynamics. Also, in the retests with pilot E the noise break frequency was 1 radian per second, and there are two series in which a cam-generated disturbance is used instead of the filtered noise generator. The cam-produced noise had a complete break off at approximately 2 radians per second. However, no consistent variation in the measured transfer function with these changes in disturbance characteristics was noted. A slight increase in closed-loop frequency with increase in noise break frequency was noted.

Also included in the retests with pilot E were two series in which a pursuit tracking task instead of the compensatory task was used. With the pursuit task a noticeable and consistent reduction in the closed-loop natural frequency is shown, but that appears to be the only change that occurs that is outside the normal variations in the results.

CONCLUSIONS

Tests in which the transfer function of human pilots has been measured show that the pilots change their transfer function whenever any element of the control loop is changed. However, fairly consistent results in terms of the

closed-loop characteristics are obtained. The pilot will adjust his transfer function so as to obtain closed-loop oscillatory characteristics with a frequency of approximately 3 radians per second and a damping ratio of from 0.4 to 0.7, with the following qualifications. With acceleration dynamics it is difficult to maintain a damping ratio of 0.4, and it is usually reduced. The characteristic frequency is reduced when the display sensitivity or control power is reduced. The real roots of the closed-loop characteristic are kept as high as possible and were usually higher than 1 radian per second. The tests indicate that the more experienced pilots operated so as to obtain the highest real roots, frequency, and damping ratio.

Langley Research Center,
National Aeronautics and Space Administration,
Langley Station, Hampton, Va., June 12, 1963.

APPENDIX A

DERIVATION OF THE GAIN ADJUSTMENT

The gain adjustment in the analog pilot used in this paper is accomplished in the following manner. Define a function of the difference between the output of the human pilot and the analog pilot

$$x = \text{Pilot output} - \text{Analog-pilot output}$$

as follows:

$$f(x) = \frac{x^2}{2}$$

The square of the difference x will be minimized if the rate of change of any particular gain in the analog pilot α is set equal to the partial derivative of the error function with respect to this gain

$$\dot{\alpha} = K \frac{\partial f}{\partial \alpha}$$

This equation can also be expressed as

$$\dot{\alpha} = K \frac{\partial f}{\partial x} \frac{\partial x}{\partial \alpha}$$

$$\dot{\alpha} = Kx \frac{\partial x}{\partial \alpha}$$

Since only the output of the analog pilot is a function of the gains to be considered and the output of the pilot is not, the statement given above can be rewritten as

$$\dot{\alpha} = Kx \frac{\partial \delta}{\partial \alpha}$$

where δ is the output of analog pilot. The particular expressions that apply to the form of the analog pilot as used in this study are as follows:

$$\frac{\delta}{I} = \frac{K_1 \tau + K_1 K_2 s}{(\tau + s)^2}$$

For K_1,

$$\frac{\partial \delta}{\partial K_1} = \left[\frac{\tau + K_2 s}{(\tau + s)^2}\right] I$$

For τ,

$$\frac{\partial \delta}{\partial \tau} = \frac{K_1 I - 2(\tau + s)\delta}{(\tau + s)^2}$$

By referring to the analog diagram of the analog pilot given below, it can be seen that the following transfer functions for intermediate positions in the diagram can be written:

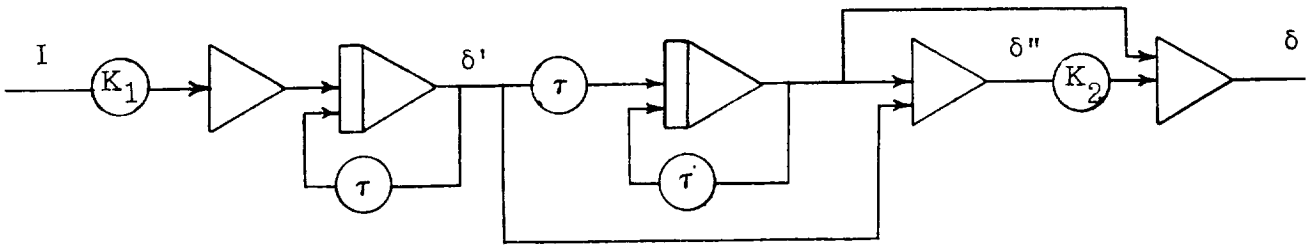

$$\frac{\delta'}{I} = \frac{K_1}{\tau + s}$$

$$\frac{\delta''}{I} = \frac{-K_1 s}{(\tau + s)^2}$$

By substituting $\frac{\delta}{I}\frac{I}{\delta'}\delta'$ for δ and $\frac{I}{\delta'}\delta'$ for I, the following expressions can be obtained:

$$\frac{\partial \delta}{\partial \tau} = \frac{\left(\frac{\tau + s}{K_1}\right)\delta' K_1 - \left[\frac{K_1\tau + K_1 K_2 s}{(\tau + s)^2}\right]\left(\frac{\tau + s}{K_1}\right)\delta'\left[2(\tau + s)\right]}{(\tau + s)^2}$$

$$= -\left[\frac{\tau + (2K_2 - 1)s}{(\tau + s)^2}\right]\delta'$$

For K_2,

$$\frac{\partial \delta}{\partial K_2} = \frac{I K_1 s}{(\tau + s)^2}$$

By substituting $\frac{I}{\delta''}\delta''$ for I, the following expression is obtained:

$$\frac{\partial\delta}{\partial K_2} = \left[\frac{(\tau + s)^2}{-K_1 s}\right]\left[\frac{K_1 s}{(\tau + s)^2}\right]\delta''$$

$$= -\delta''$$

A complete computer diagram of the mechanization of the analog pilot and the gain adjustment derived above is shown in figure 26. Computer diagrams for the controlled dynamics used in the tests are shown in figure 27.

APPENDIX B

DERIVATION OF CLOSED-LOOP TRANSFER FUNCTIONS

An example of the derivation of the closed-loop transfer function for a case in which the function relating pilot output to the disturbance by using the oscillatory dynamics is given.

$$\frac{\delta}{D} = \frac{K_1\tau\left(1 + \frac{K_2}{\tau}s\right)}{(\tau + s)^2}$$

$$\frac{\theta}{\delta} = \frac{10}{s^2 + 3s + 10}$$

therefore,

$$\frac{\theta}{D} = \frac{10K_1\tau\left(1 + \frac{K_2}{\tau}s\right)}{\left(s^2 + 3s + 10\right)(\tau + s)^2}$$

where

δ analog pilot output

D disturbance

θ system output

An example for the case where the function relating pilot output to displayed error by using the rate dynamics is given

$$\frac{\delta}{\epsilon} = \frac{K_1\tau\left(1 + \frac{K_2}{\tau}s\right)}{(\tau + s)^2}$$

$$\frac{\theta}{\delta} = \frac{2}{s}$$

$$\epsilon = D - \theta$$

therefore

$$\frac{\theta}{D} = \frac{2K_1\tau\left(1 + \frac{K_2}{\tau}s\right)}{s^3 + 2\tau s^2 + \left(\tau^2 + 2K_1K_2\right)s + 2K_1\tau}$$

where ϵ is the displayed error.

REFERENCES

1. Adams, James J.: A Simplified Method for Measuring Human Transfer Functions. NASA TN D-1782, 1963.

2. Kuehnel, Helmut A.: Human Pilots' Dynamic-Response Characteristics Measured in Flight and on a Nonmoving Simulator. NASA TN D-1229, 1962.

3. Hall, Ian A. M.: Effects of Controlled Element on the Human Pilot. WADC Tech. Rep. 57-509 (ASTIA Doc. No. AD 130979), U.S. Air Force, Aug. 1958.

4. McRuer, Duane T., and Krendel, Ezra S.: The Human Operator as a Servo System Element. Jour. Franklin Inst.
   Pt. I, vol. 267, no. 5, May 1959, pp. 381-403.
   Pt. II, vol. 267, no. 6, June 1959, pp. 511-536.

5. Seckel, Edward, Hall, Ian A. M., McRuer, Duane T., and Weir, David H.: Human Pilot Dynamic Response in Flight and Simulator. WADC Tech. Rep. 57-520, ASTIA Doc. No. AD 130988, U.S. Air Force, Aug. 1958.

6. Elkind, Jerome I.: Characteristics of Simple Manual Control Systems. Tech. Rep. No. 111, Lincoln Lab., M.I.T., Apr. 6, 1956.

7. Osburn, P. V., Whitaker, H. P., and Kezer, A.: New Developments in the Design of Model Reference Adaptive Control Systems. Paper No. 61-39, Inst. Aerospace Sci., Jan. 1961.

TABLE I.- SUMMARY OF DATA

(a) Pilot A

Dynamics	Disturbance break frequency, radians/sec	Measured gains			Transfer function	$\frac{\theta}{D}$ characteristics		
		K_1	τ, radians/sec	K_2		ω, radians/sec	ζ	Real roots
1	1	8	8	0	$\frac{\delta}{D} = \frac{1}{(1 + 0.12s)^2}$			
$\frac{1}{s + 1}$	1	5.5	6.5	7	$\frac{\delta}{D} = \frac{0.85(1 + 1.08s)}{(1 + 0.15s)^2}$			
$\frac{10}{s^2 + 3s + 10}$	2	5.5	12.5	9	$\frac{\delta}{D} = \frac{0.44(1 + 0.72s)}{(1 + 0.08s)^2}$			
$\frac{2}{s}$	1	8	4.5	2	$\frac{\delta}{\epsilon} = \frac{1.77(1 + 0.44s)}{(1 + 0.22s)^2}$	6.25	0.57	-1.8
$\frac{2}{s}$	.5	7	5	1.5	$\frac{\delta}{\epsilon} = \frac{1.4(1 + 0.33s)}{(1 + 0.2s)^2}$	5.1	.71	-2.63
$\frac{10}{s(s + 1)}$	.5	23	17	4.5	$\frac{\delta}{\epsilon} = \frac{1.35(1 + 0.26s)}{(1 + 0.06s)^2}$	4.79	.37	-8.19,-23.2
$\frac{10}{s^2}$	.5	21	16.5	4.5	$\frac{\delta}{\epsilon} = \frac{1.27(1 + 0.27s)}{(1 + 0.06s)^2}$	4.25	.23	-8.57,-22.4

(b) Pilot B

Dynamics	Disturbance break frequency, radians/sec	Measured gains			Transfer function	$\frac{\theta}{D}$ characteristics		
		K_1	τ, radians/sec	K_2		ω, radians/sec	ζ	Real roots
1	1	6.5	7	0	$\frac{\delta}{D} = \frac{0.93}{(1 + 0.14s)^2}$			
$\frac{1}{s + 1}$	1	3	4	5	$\frac{\delta}{D} = \frac{0.75(1 + 1.25s)}{(1 + 0.25s)^2}$			
$\frac{4}{s}$	1	5	3	1	$\frac{\delta}{\epsilon} = \frac{1.6(1 + 0.33s)}{(1 + 0.33s)^2}$	4.48	0.34	-3
$\frac{4}{s}$	.5	6.5	4	0	$\frac{\delta}{\epsilon} = \frac{1.63}{(1 + 0.25s)^2}$	4.0	.4	-7.68
$\frac{10}{s(s + 1)}$	.25	5	10	3	$\frac{\delta}{\epsilon} = \frac{0.5(1 + 0.3s)}{(1 + 0.1s)^2}$	2.46	.32	-6.35,-13.0
$\frac{10}{s^2}$	.25	8	15	5	$\frac{\delta}{\epsilon} = \frac{0.53(1 + 0.33s)}{(1 + 0.06s)^2}$	2.5	.22	-9.6,-19.2

TABLE I.- SUMMARY OF DATA - Continued

(c) Pilot C

Dynamics	Disturbance break frequency, radians/sec	Measured gains			Transfer function	$\frac{\theta}{D}$ characteristics		
		K_1	τ, radians/sec	K_2		ω, radians/sec	ζ	Real roots
1	1	9	11	0	$\frac{\delta}{D} = \frac{0.82}{(1 + 0.09s)^2}$			
$\frac{1}{1 + s}$	1	5.5	6	3	$\frac{\delta}{D} = \frac{0.72(1 + 0.5s)}{(1 + 0.17s)^2}$			
$\frac{10}{s^2 + 3s + 10}$	1	8	10.5	2.5	$\frac{\delta}{D} = \frac{0.76(1 + 0.24s)}{(1 + 0.09s)^2}$			
$\frac{2}{s}$	.5	10	9	0	$\frac{\delta}{\epsilon} = \frac{1.1}{(1 + 0.11s)^2}$	3.76	0.69	-12.76
$\frac{10}{s(s + 1)}$	.5	10	14	3.5	$\frac{\delta}{\epsilon} = \frac{0.71(1 + 0.25s)}{(1 + 0.07s)^2}$	2.98	.32	-9.1,-18.0
$\frac{10}{s^2}$	.5	10	20	4	$\frac{\delta}{\epsilon} = \frac{0.5(1 + 0.2s)}{(1 + 0.05s)^2}$	2.33	.11	-15.8,-23.6

(d) Pilot D

Dynamics	Disturbance break frequency, radians/sec	Measured gains			Transfer function	$\frac{\theta}{D}$ characteristics		
		K_1	τ, radians/sec	K_2		ω, radians/sec	ζ	Real roots
1	1	5	5.5	0.5	$\frac{\delta}{D} = \frac{0.91(1 + 0.09s)}{(1 + 0.18s)^2}$			
$\frac{1}{s + 1}$	1	3	3.5	4.5	$\frac{\delta}{D} = \frac{0.86(1 + 1.3s)}{(1 + 0.29s)^2}$			
$\frac{4}{s}$	1	5	7	0	$\frac{\delta}{\epsilon} = \frac{0.71}{(1 + 0.14s)^2}$	3.6	0.47	-10.6
$\frac{4}{s}$	.5	4	7	0	$\frac{\delta}{\epsilon} = \frac{0.57}{(1 + 0.14s)^2}$	3.3	.56	-10.3
$\frac{10}{s(s + 1)}$	.5	2	5.5	5	$\frac{\delta}{\epsilon} = \frac{0.36(1 + 0.91s)}{(1 + 0.18s)^2}$	3.3	.3	-1.13,-8.8
$\frac{10}{s^2}$	.5	4	9	5	$\frac{\delta}{\epsilon} = \frac{0.44(1 + 0.56s)}{(1 + 0.11s)^2}$	2.76	.28	-3.73,-12.7

TABLE I.- SUMMARY OF DATA - Continued

(e) Pilot E

Dynamics	Disturbance break frequency, radians/sec	Measured gains			Transfer function	$\frac{\theta}{D}$ characteristics		
		K_1	τ, radians/sec	K_2		ω, radians/sec	ζ	Real roots
1	1	9	10	0	$\frac{\delta}{D} = \frac{0.9}{(1 + 0.1s)^2}$			
$\frac{1}{s + 1}$	1	4	3.5	4	$\frac{\delta}{D} = \frac{1.14(1 + 1.14s)}{(1 + 0.29s)^2}$			
$\frac{10}{s^2 + 3s + 10}$	1	3.5	6.5	2	$\frac{\delta}{D} = \frac{0.54(1 + 0.31s)}{(1 + 0.15s)^2}$			
$\frac{2}{s}$	.5	2	3	2	$\frac{\delta}{\epsilon} = \frac{0.7(1 + 0.67s)}{(1 + 0.33s)^2}$	3.46	0.72	-1.0
$\frac{10}{s(s + 1)}$	.5	4.5	9	3.5	$\frac{\delta}{\epsilon} = \frac{0.5(1 + 0.39s)}{(1 + 0.11s)^2}$	2.6	.39	-4.76,-12.2
$\frac{10}{s^2}$	.5	7	14	5	$\frac{\delta}{\epsilon} = \frac{0.5(1 + 0.36s)}{(1 + 0.071s)^2}$	2.5	.23	-8.8,-18.0

(f) Pilot F

Dynamics	Disturbance break frequency, radians/sec	Measured gains			Transfer function	$\frac{\theta}{D}$ characteristics		
		K_1	τ, radians/sec	K_2		ω, radians/sec	ζ	Real roots
1	1	3	4	1	$\frac{\delta}{D} = \frac{0.75(1 + 0.25s)}{(1 + 0.25s)^2}$			
$\frac{1}{s + 1}$	1	2.5	6	4	$\frac{\delta}{D} = \frac{0.42(1 + 0.67s)}{(1 + 0.167s)^2}$			
$\frac{10}{s^2 + 3s + 10}$	1	5	8	2	$\frac{\delta}{D} = \frac{0.62(1 + 0.25s)}{(1 + 0.125s)^2}$			
$\frac{2}{s}$	1	3.5	3.5	1.5	$\frac{\delta}{\epsilon} = \frac{1(1 + 0.43s)}{(1 + 0.29s)^2}$	3.64	0.71	-1.85
$\frac{10}{s(s + 1)}$	1	.75	3	6	$\frac{\delta}{\epsilon} = \frac{0.25(1 + 2.0s)}{(1 + 0.33s)^2}$	3.02	.11	-5.9,-4.64
$\frac{10}{s^2}$	1	.75	4.5	8	$\frac{\delta}{\epsilon} = \frac{0.167(1 + 1.78s)}{(1 + 0.22s)^2}$	2.63	.20	-0.67,-7.2

TABLE I.- SUMMARY OF DATA - Concluded

(g) Engineer G

Dynamics	Disturbance break frequency, radians/sec	Measured gains			Transfer function	$\frac{\theta}{D}$ characteristics		
		K_1	τ, radians/sec	K_2		ω, radians/sec	ζ	Real roots
1	1	5.5	6	0.5	$\frac{\delta}{D} = \frac{0.92(1 + 0.08s)}{(1 + 0.167s)^2}$			
$\frac{1}{s + 1}$	1	3	4.5	3	$\frac{\delta}{D} = \frac{0.67(1 + 0.67s)}{(1 + 0.22s)^2}$			
$\frac{2}{s}$	.5	2	2	3.5	$\frac{\delta}{\epsilon} = \frac{1(1 + 1.75s)}{(1 + 0.5s)^2}$	4.04	0.40	-0.49
$\frac{10}{s(s + 1)}$	.5	2	6	9	$\frac{\delta}{\epsilon} = \frac{0.33(1 + 1.5s)}{(1 + 0.16s)^2}$	4.32	.25	-0.63,-10.1
$\frac{10}{s^2}$	.5	4.5	8	7	$\frac{\delta}{\epsilon} = \frac{0.56(1 + 0.87s)}{(1 + 0.12s)^2}$	4.46	.20	-1.42,-12.74

(h) Engineer H

Dynamics	Disturbance break frequency, radians/sec	Measured gains			Transfer function	$\frac{\theta}{D}$ characteristics		
		K_1	τ, radians/sec	K_2		ω, radians/sec	ζ	Real roots
1	1	3	3	1	$\frac{\delta}{D} = \frac{1(1 + 0.33s)}{(1 + 0.33s)^2}$			
$\frac{1}{s + 1}$	1	8	8	8	$\frac{\delta}{D} = \frac{1(1 + 1s)}{(1 + 0.125s)^2}$			
$\frac{10}{s^2 + 3s + 10}$	1	6	10	4	$\frac{\delta}{D} = \frac{0.6(1 + 0.4s)}{(1 + 0.1s)^2}$			
$\frac{2}{s}$	1	8.5	3.5	1.5	$\frac{\delta}{\epsilon} = \frac{2.4(1 + 0.43s)}{(1 + 0.29s)^2}$	5.25	0.46	-2.16
$\frac{10}{s(s + 1)}$	1	5	6.5	5.5	$\frac{\delta}{\epsilon} = \frac{0.77(1 + 0.85s)}{(1 + 0.15s)^2}$	4.87	.14	-1.21,-11.38
$\frac{10}{s^2}$	1	5	8	8	$\frac{\delta}{\epsilon} = \frac{0.62(1 + 1s)}{(1 + 0.125s)^2}$	5.1	.15	-1.15,-13.3

TABLE II.- SUMMARY OF DATA

(a) Second test of Pilot E

[Disturbance break frequency, 1 radian/sec]

Test	Dynamics	Measured gains			Transfer function	$\frac{\theta}{D}$ characteristics			Root-mean-square error, volts
						Oscillatory		Real roots	
		K_1	τ, radians/sec	K_2		ω, radians/sec	ζ		
1	1	1	1.5	2.5	$\frac{\delta}{D} = \frac{0.66(1 + 1.67s)}{(1 + 0.66s)^2}$				0.6
2	$\frac{1}{1 + s}$	4	4	4	$\frac{\delta}{D} = \frac{1(1 + 1s)}{(1 + 0.25s)^2}$				1.0
3	$\frac{10}{s^2 + 3s + 10}$	4	5.5	2	$\frac{\delta}{D} = \frac{0.72(1 + 0.36s)}{(1 + 0.18s)^2}$				1.1
4	$\frac{10}{s(s + 1)}$	2.5	6	3.5	$\frac{\delta}{\epsilon} = \frac{0.42(1 + 0.58s)}{(1 + 0.16s)^2}$	3.34	0.49	-0.514, -9.16	1.7
5	$\frac{10}{s^2}$	8.5	11	4	$\frac{\delta}{\epsilon} = \frac{0.77(1 + 0.36s)}{(1 + 0.09s)^2}$	3.35	.19	-5.44, -15.2	3.6

(b) Third test of Pilot E

[Disturbance break frequency, 1 radian/sec]

Test	Dynamics	Measured gains			Transfer function	$\frac{\theta}{D}$ characteristics			Root-mean-square error, volts
						Oscillatory		Real roots	
		K_1	τ, radians/sec	K_2		ω, radians/sec	ζ		
1	1	4	4.5	0.5	$\frac{\delta}{D} = \frac{0.89(1 + 0.11s)}{(1 + 0.22s)^2}$				0.6
2	$\frac{1}{s + 1}$	6	6	5	$\frac{\delta}{D} = \frac{1(1 + 0.83s)}{(1 + 0.16s)^2}$				1.1
3	$\frac{10}{s^2 + 3s + 10}$	4.5	7	1.5	$\frac{\delta}{D} = \frac{0.64(1 + 0.21s)}{(1 + 0.14s)^2}$				1.0
4	$\frac{2}{s}$	4	3	2	$\frac{\delta}{\epsilon} = \frac{1.3(1 + 0.67s)}{(1 + 0.33s)^2}$	4.36	0.54	-1.26	.7
5	$\frac{10}{s(s + 2.5)}$	3	5	2	$\frac{\delta}{\epsilon} = \frac{0.6(1 + 0.4s)}{(1 + 0.2s)^2}$	2.8	.40	-2.5, -7.78	1.2
6	$\frac{10}{s(s + 1)}$	2.5	6.5	5.5	$\frac{\delta}{\epsilon} = \frac{0.38(1 + 0.83s)}{(1 + 0.15s)^2}$	3.45	.37	-1.24, -10.1	1.6
7	$\frac{10}{s^2}$	4	9.5	8	$\frac{\delta}{\epsilon} = \frac{0.42(1 + 0.84s)}{(1 + 0.10s)^2}$	3.9	.40	-1.41, -1.78	2.0
8	$\frac{10}{s(s^2 + 3s + 10)}$	6	7	5	$\frac{\delta}{\epsilon} = \frac{0.86(1 + 0.71s)}{(1 + 0.14s)^2}$	3.2, 7.9	0.18, 0.96	-0.60	1.6

TABLE II.- SUMMARY OF DATA - Continued

(c) Fourth test of Pilot E

[Disturbance break frequency, 1 radian/sec]

Test	Dynamics	Measured gains			Transfer function	$\frac{\theta}{D}$ characteristics			Root-mean-square error, volts
						Oscillatory		Real roots	
		K_1	τ, radians/sec	K_2		ω, radians/sec	ζ		
4	$\frac{10}{s^2 + 3s + 10}$	3.5	6.5	2	$\frac{\delta}{D} = \frac{0.54(1 + 0.31s)}{(1 + 0.15s)^2}$				
3	$\frac{2}{s}$	2	4	1.5	$\frac{\delta}{\epsilon} = \frac{0.5(1 + 0.37s)}{(1 + 0.25s)^2}$	3.78	0.91	-1.12	1.4
2	$\frac{10}{s(s + 1)}$	3	6.5	6.5	$\frac{\delta}{\epsilon} = \frac{0.46(1 + 1s)}{(1 + 0.15s)^2}$	4.39	.29	-0.61,-10.8	1.5
1	$\frac{10}{s^2}$	3	7	6.5	$\frac{\delta}{\epsilon} = \frac{0.43(1 + 0.93s)}{(1 + 0.14s)^2}$	3.71	.21	-1.38,-10.9	2.2

(d) Fifth test of Pilot E

[Cam-generated disturbance]

Test	Dynamics	Measured gains			Transfer function	$\frac{\theta}{D}$ characteristics			Root-mean-square error, volts
						Oscillatory		Real roots	
		K_1	τ, radians/sec	K_2		ω, radians/sec	ζ		
1	1	4	4.5	1	$\frac{\delta}{D} = \frac{0.89(1 + 0.22s)}{(1 + 0.22s)^2}$				1.0
2	$\frac{1}{s + 1}$	4.5	5	5.5	$\frac{\delta}{D} = \frac{0.9(1 + 1.1s)}{(1 + 0.2s)^2}$				1.1
3	$\frac{10}{s^2 + 3s + 10}$	4	7	3	$\frac{\delta}{D} = \frac{0.57(1 + 0.43s)}{(1 + 0.14s)^2}$				1.1
4	$\frac{2}{s}$	5.5	3.5	1.5	$\frac{\delta}{\epsilon} = \frac{1.57(1 + 0.43s)}{(1 + 0.29s)^2}$	4.3	0.57	-2.08	1.0
5	$\frac{10}{s(s + 1)}$	2.5	5	4	$\frac{\delta}{\epsilon} = \frac{0.5(1 + 0.8s)}{(1 + 0.2s)^2}$	3.6	.28	-0.45,-8.53	1.4
6	$\frac{10}{s^2}$	2.5	6	5.5	$\frac{\delta}{\epsilon} = \frac{0.42(1 + 0.92s)}{(1 + 0.17s)^2}$	3.3	.15	-1.39,-9.57	1.6

TABLE II.- SUMMARY OF DATA - Concluded

(e) Sixth test of Pilot E; pursuit tracking

[Disturbance break frequency, 1 radian/sec]

Test	Dynamics	Measured gains			Transfer function	$\frac{\theta}{D}$ characteristics			Root-mean-square error, volts
						Oscillatory		Real roots	
		K_1	τ, radians/sec	K_2		ω, radians/sec	ζ		
6	1	3	4	0	$\frac{\delta}{D} = \frac{0.75}{(1 + 0.25s)^2}$				1.1
5	$\frac{1}{s + 1}$	3.5	4	4	$\frac{\delta}{D} = \frac{0.88(1 + 1s)}{(1 + 0.25s)^2}$				1.2
4	$\frac{10}{s^2 + 3s + 10}$	3	5	1.5	$\frac{\delta}{D} = \frac{0.6(1 + 0.3s)}{(1 + 0.2s)^2}$				1.4
3	$\frac{2}{s}$	4	4	.5	$\frac{\delta}{\epsilon} = \frac{1(1 + 0.12s)}{(1 + 0.25s)^2}$	2.4	0.54	-5.39	1.4
2	$\frac{10}{s(s + 1)}$	1.5	4.5	4	$\frac{\delta}{\epsilon} = \frac{0.33(1 + 0.9s)}{(1 + 0.22s)^2}$	3.1	.35	-0.38,-7.45	1.7
1	$\frac{10}{s^2}$	1	5	5.5	$\frac{\delta}{\epsilon} = \frac{0.2(1 + 1.1s)}{(1 + 0.2s)^2}$	2.2	.25	-1.35,-7.53	

(f) Seventh test of Pilot E; pursuit tracking

[Cam-generated disturbance]

Test	Dynamics	Measured gains			Transfer function	$\frac{\theta}{D}$ characteristics			Root-mean-square error, volts
						Oscillatory		Real roots	
		K_1	τ, radians/sec	K_2		ω, radians/sec	ζ		
4	$\frac{10}{s^2 + 3s + 10}$	5	7.5	2	$\frac{\delta}{D} = \frac{0.67(1 + 0.27s)}{(1 + 0.13s)^2}$				0.7
3	$\frac{2}{s}$	4	2.5	1	$\frac{\delta}{\epsilon} = \frac{1.6(1 + 0.4s)}{(1 + 0.4s)^2}$	2.8	0.53	-3.0	.8
2	$\frac{10}{s(s + 1)}$	3	7	5	$\frac{\delta}{\epsilon} = \frac{0.43(1 + 0.7s)}{(1 + 0.14s)^2}$	3.5	.38	-1.58,-10.7	1.1
1	$\frac{10}{s^2}$	2.5	7.5	5.5	$\frac{\delta}{\epsilon} = \frac{0.33(1 + 0.73s)}{(1 + 0.13s)^2}$	3.0	.28	-2.18,-11.1	1.5

TABLE III.- EFFECT OF DISPLAY SENSITIVITY

[Dynamics, $\frac{10}{s(s+1)}$; disturbance break frequency, 1 radian/sec; pilot E]

Display sensitivity	Measured gains			Transfer function	$\frac{\theta}{D}$ characteristics			Root-mean-square error, volts
	K_1	τ, radians/sec	K_2		Oscillatory		Real roots	
					ω, radians/sec	ζ		
1.25 v/inch	5.5	8	5.5	$\frac{\delta}{\epsilon} = \frac{0.69(1 + 0.69s)}{(1 + 0.125s)^2}$	4.66	0.28	-1.58,-12.7	1.45
5 v/inch	2.5	6.5	5.5	$\frac{\delta}{\epsilon} = \frac{0.38(1 + 0.83s)}{(1 + 0.15s)^2}$	3.45	.37	-1.24,-10.1	1.6
50 v/inch	1	6	5	$\frac{\delta}{\epsilon} = \frac{0.17(1 + 0.83s)}{(1 + 0.17s)^2}$	2.17	.70	-1.51,-8.41	2.6

TABLE IV.- EFFECT OF CONTROL SENSITIVITY

[Disturbance break frequency, 1 radian/sec; pilot E]

Dynamics	Measured gains			Transfer function	$\frac{\theta}{D}$ characteristics			Root-mean-square error, volts
	K_1	τ, radians/sec	K_2		Oscillatory		Real roots	
					ω, radians/sec	ζ		
$\frac{10}{s(s+1)}$	2.5	6.5	5.5	$\frac{\delta}{\epsilon} = \frac{0.38(1 + 0.83s)}{(1 + 0.15s)^2}$	3.45	0.37	-1.24,-10.1	1.5
$\frac{5}{s(s+1)}$	4.5	6	5	$\frac{\delta}{\epsilon} = \frac{0.75(1 + 0.83s)}{(1 + 0.17s)^2}$	3.36	.34	-1.26,-9.41	1.5
$\frac{2}{s(s+1)}$	4	4.5	3.5	$\frac{\delta}{\epsilon} = \frac{0.89(1 + 0.78s)}{(1 + 0.22s)^2}$	1.89	.23	-2.77,-6.34	1.4
$\frac{1}{s(s+1)}$	8.5	5	2.5	$\frac{\delta}{\epsilon} = \frac{1.7(1 + 0.5s)}{(1 + 0.2s)^2}$	1.44	.44	-3.11,-6.62	1.6

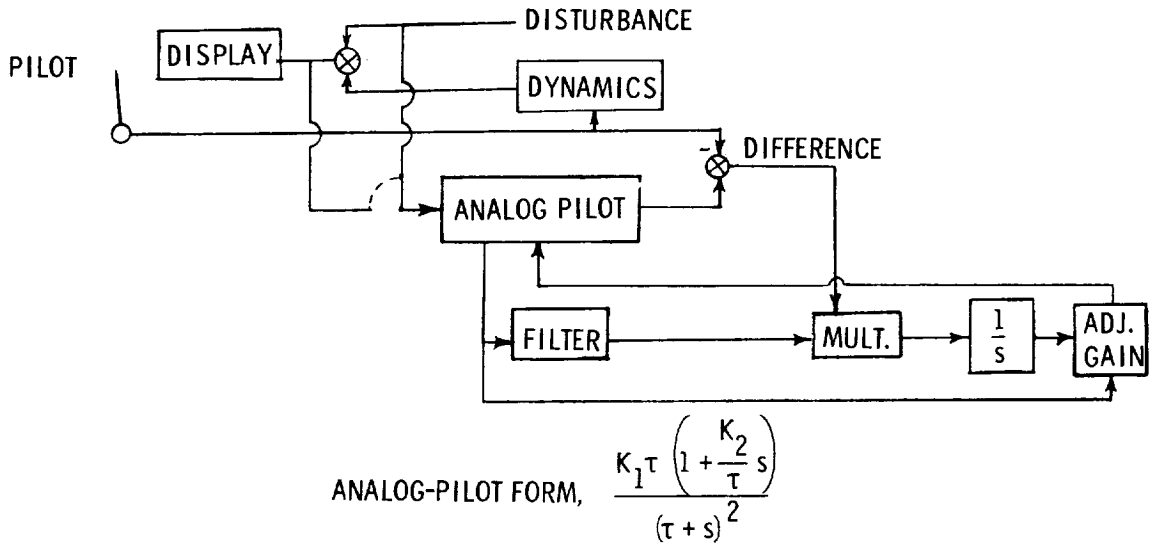

Figure 1.- Block diagram of test equipment.

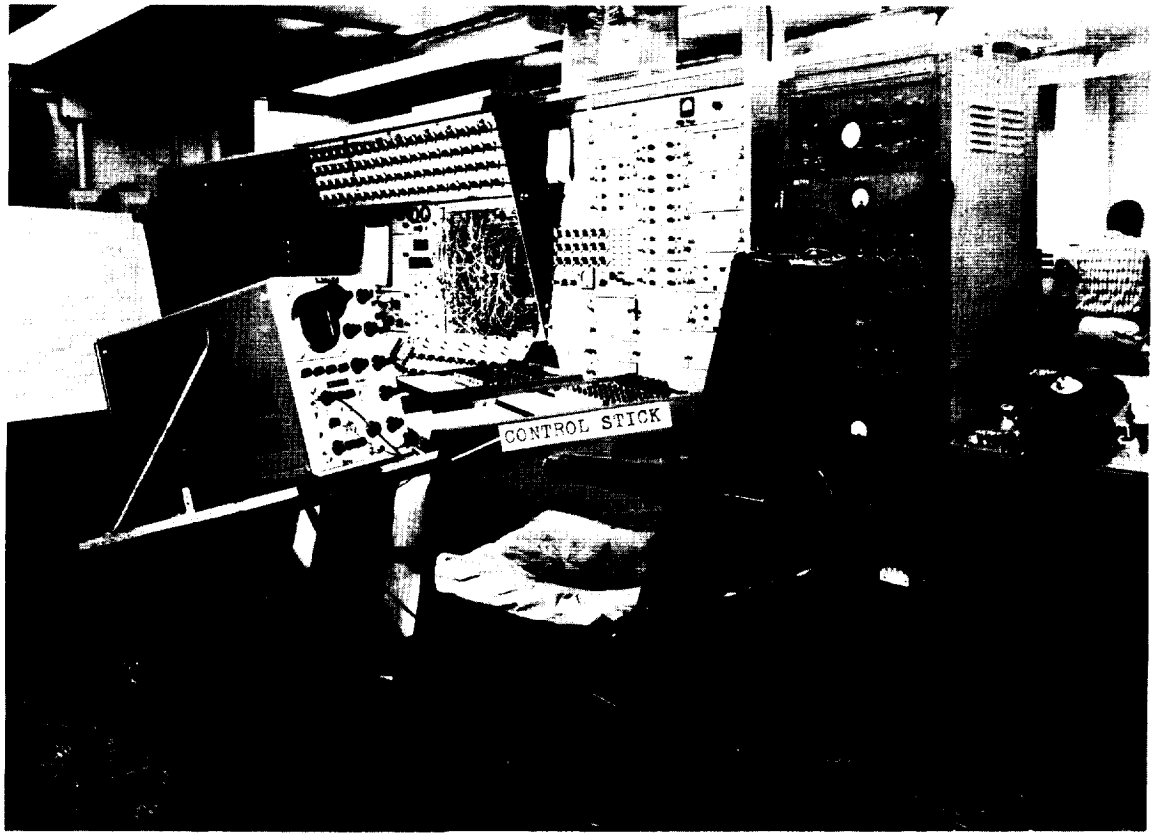

L-62-7541.1

Figure 2.- Simulator and computer used in tests.

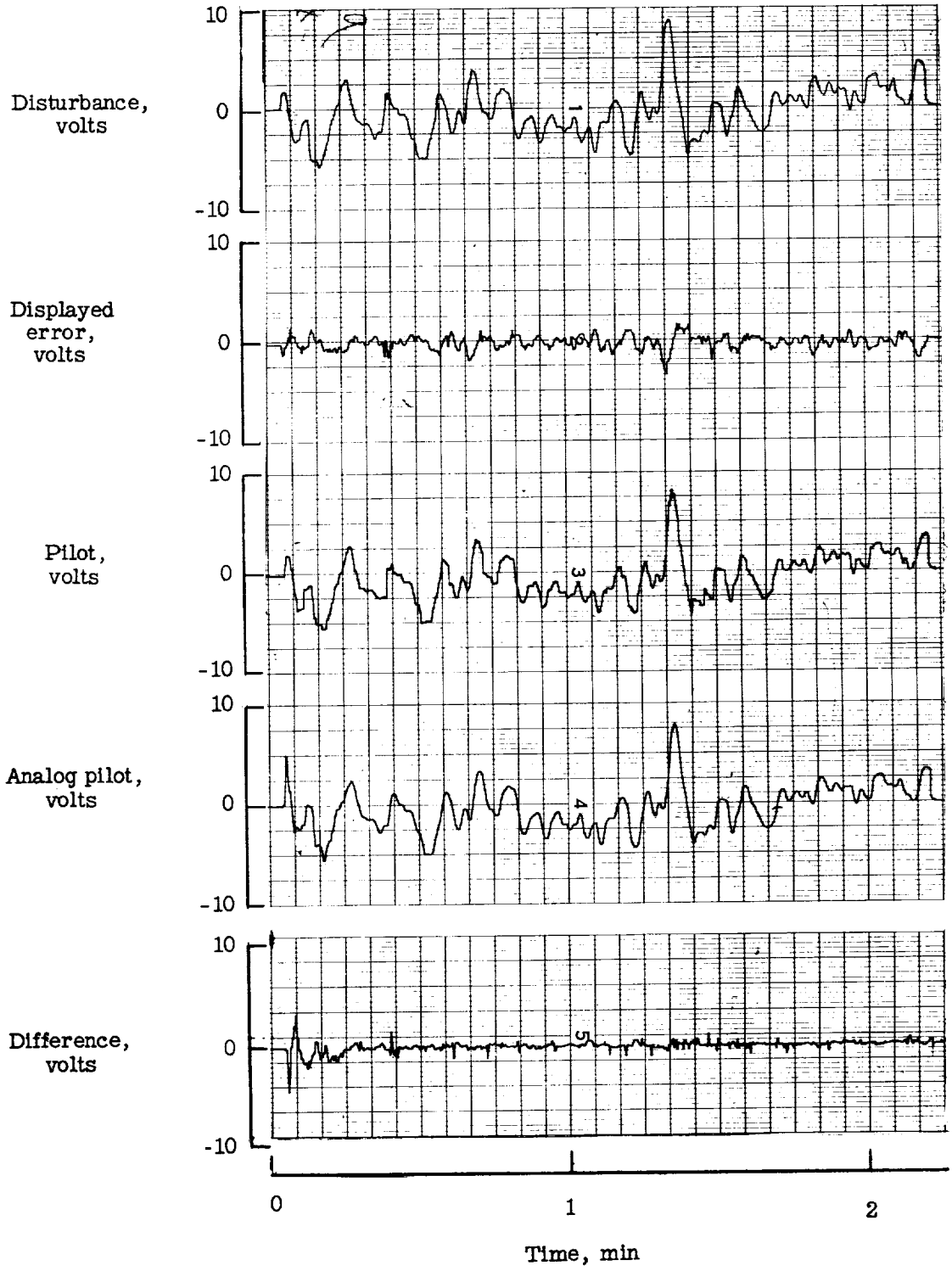

Figure 3.- Sample run with pilot E. Dynamics 1.

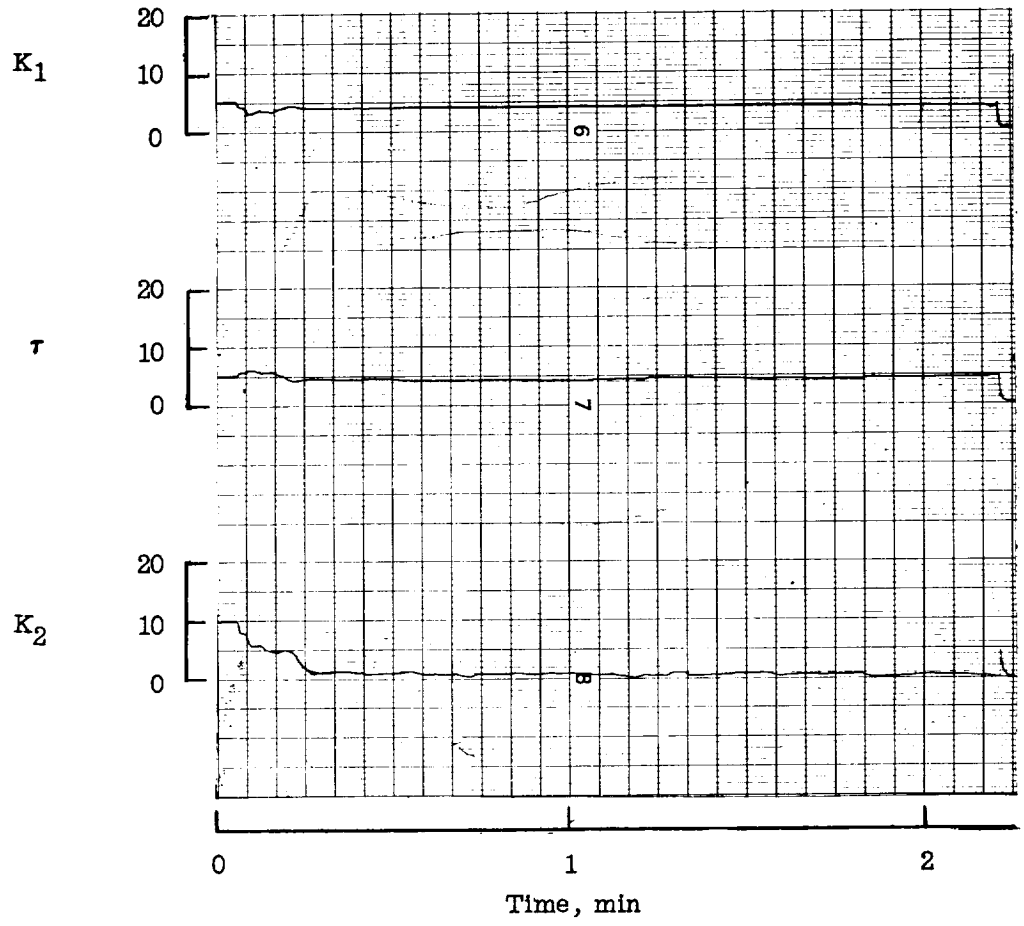

Figure 3.- Concluded.

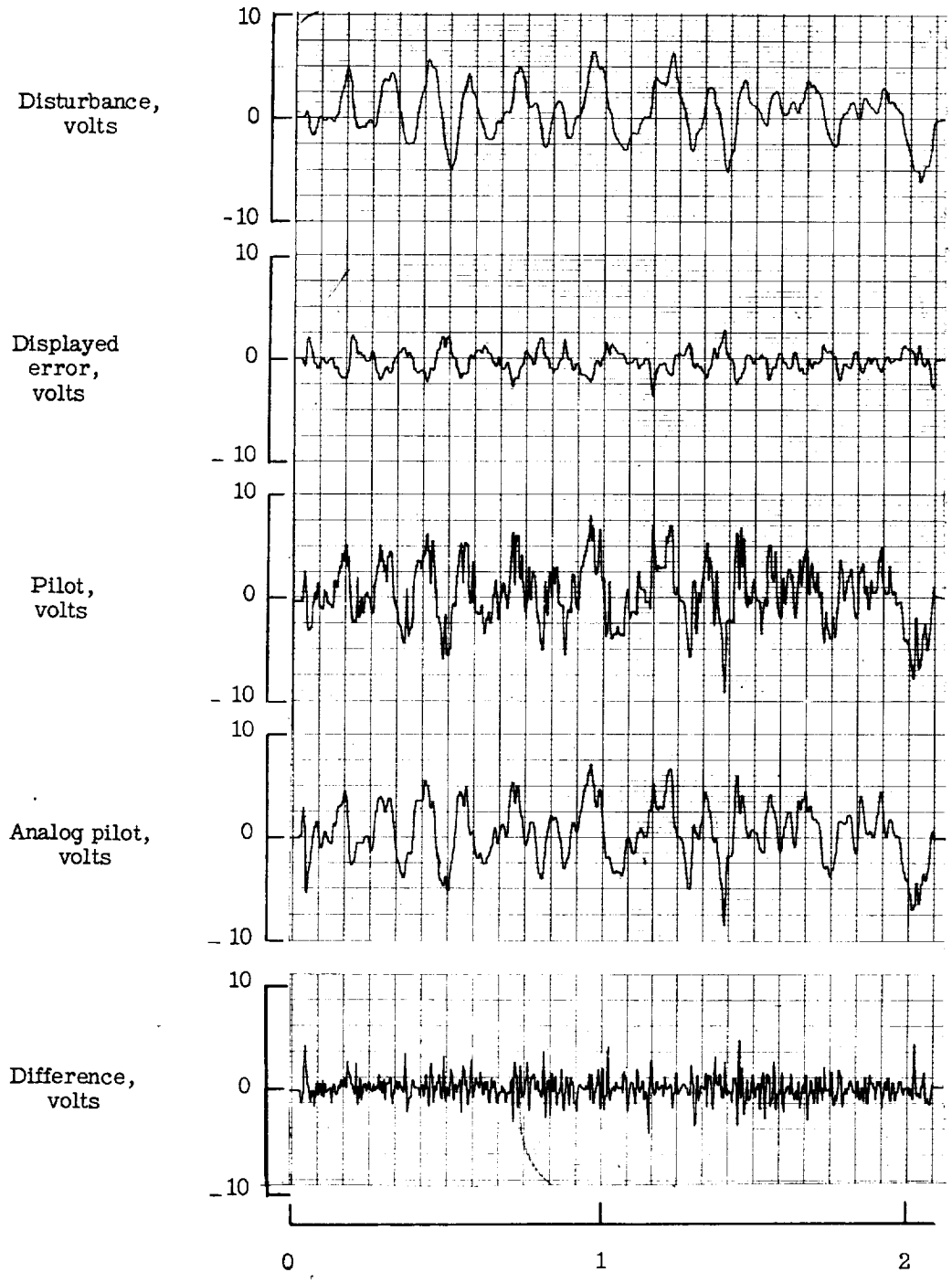

Figure 4.- Sample run with pilot E. Dynamics $\frac{1}{1 + s}$.

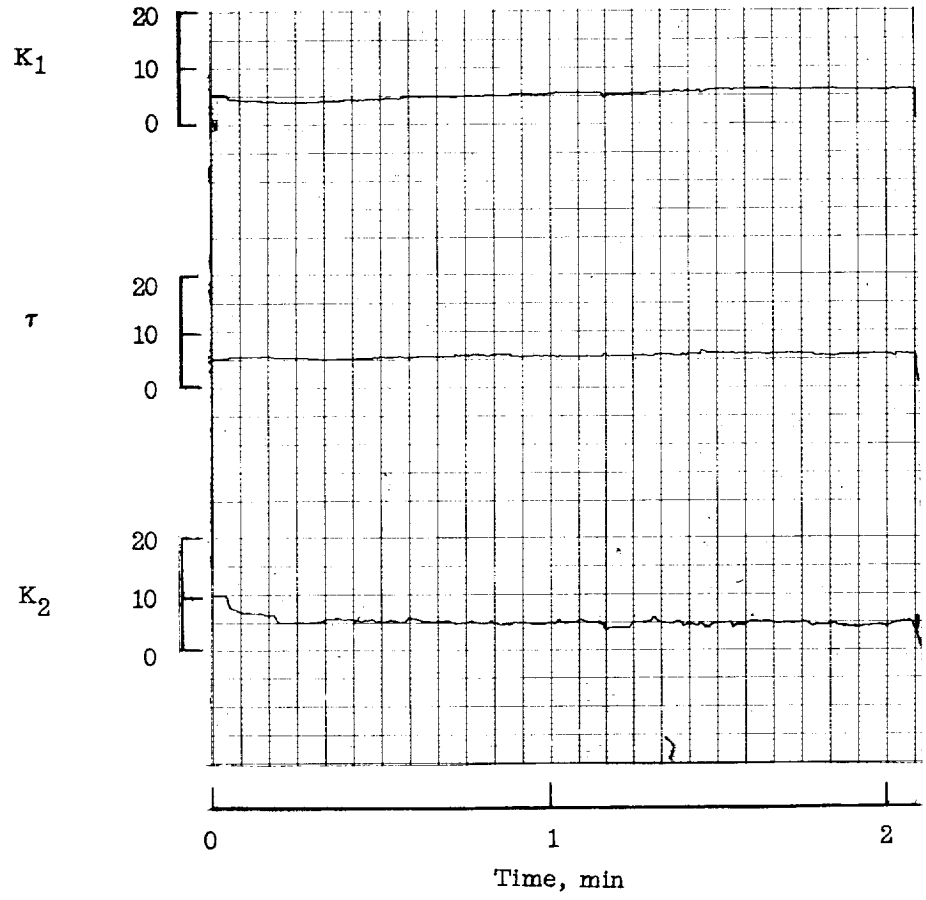

Figure 4.- Concluded.

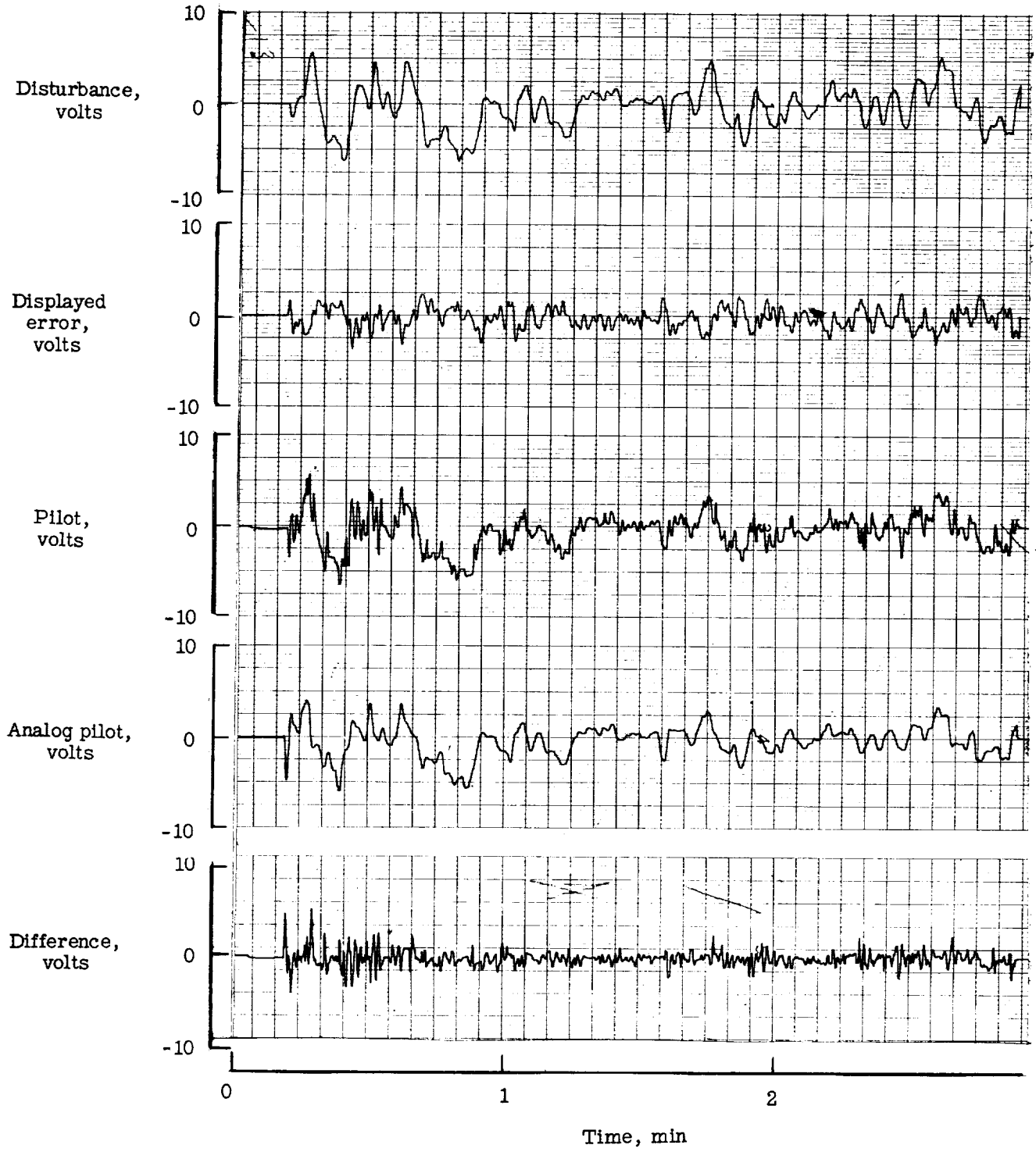

Figure 5.- Sample run with pilot E. Dynamics $\frac{10}{s^2 + 3s + 10}$.

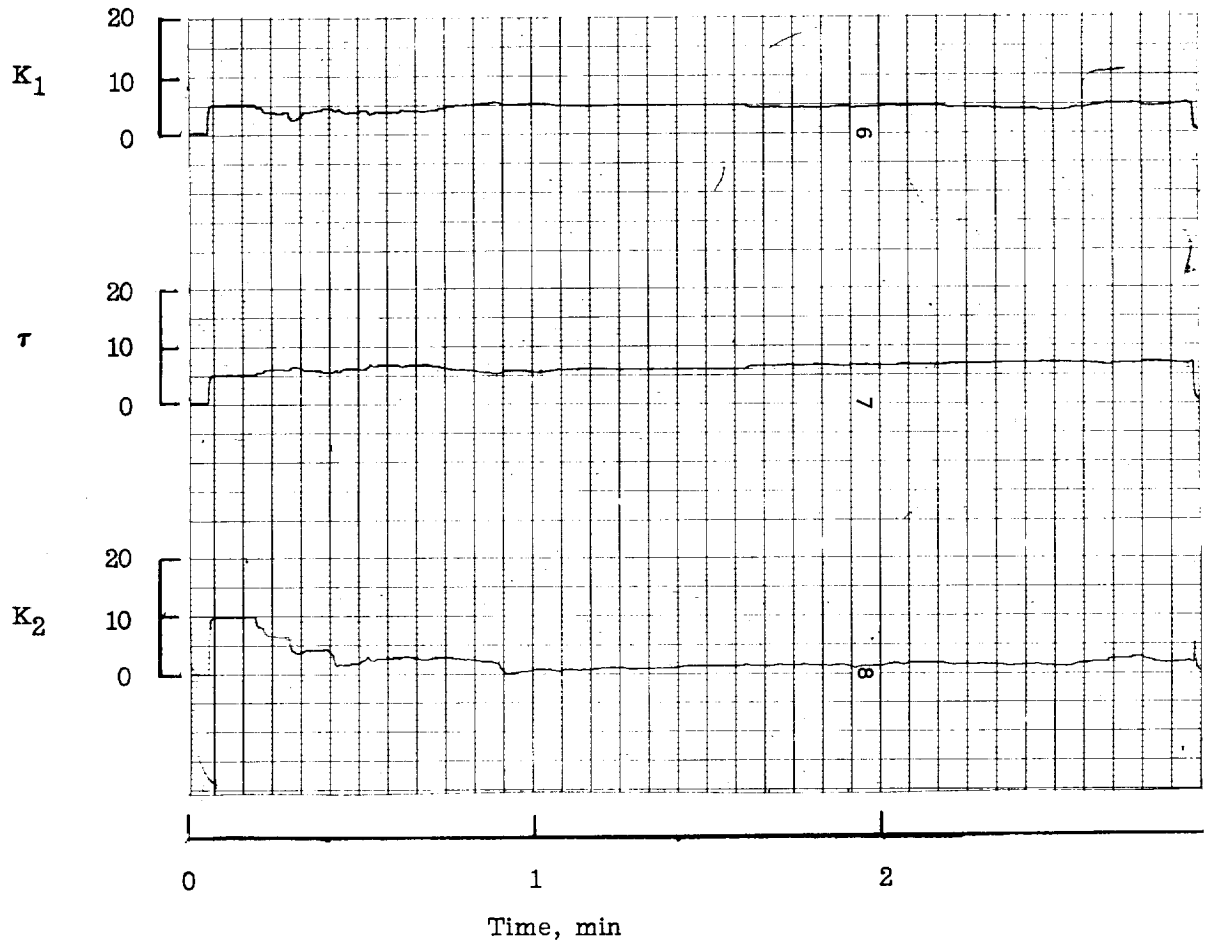

Figure 5.- Concluded.

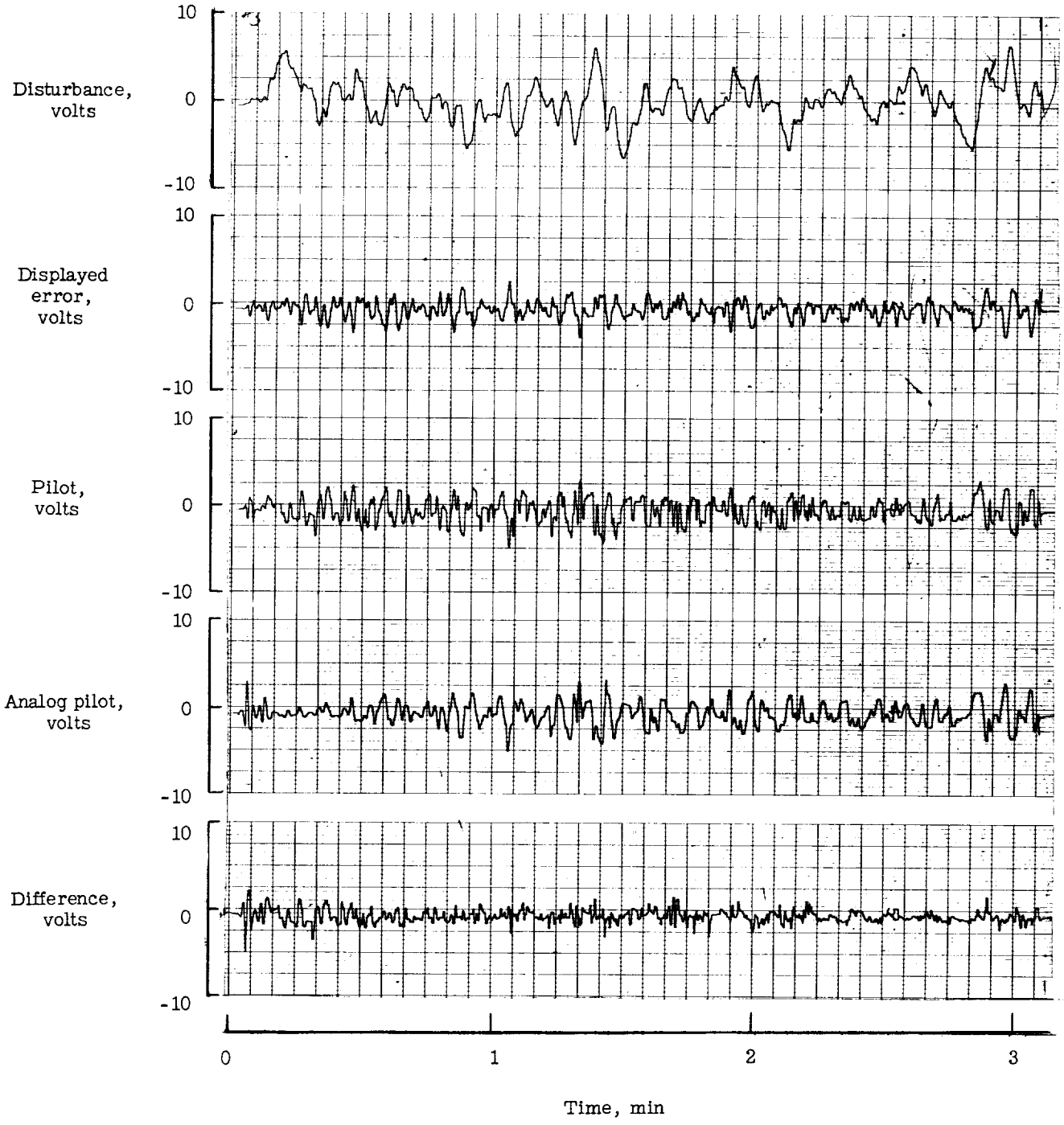

Figure 6.- Sample run with pilot E. Dynamics $\frac{2}{s}$.

Figure 6.- Concluded.

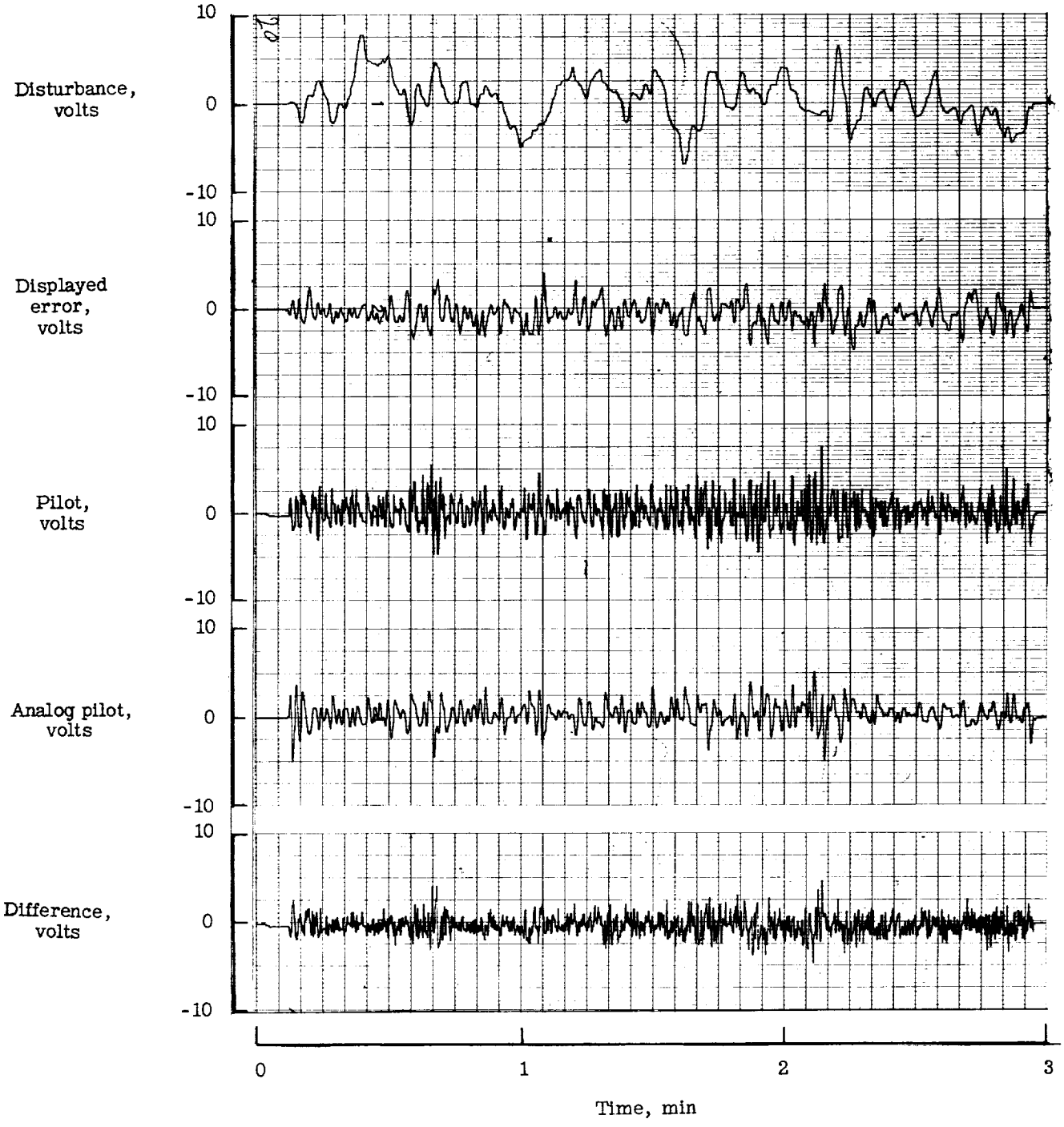

Figure 7.- Sample run with pilot E. Dynamics $\frac{10}{s(s + 1)}$.

Figure 7.- Concluded.

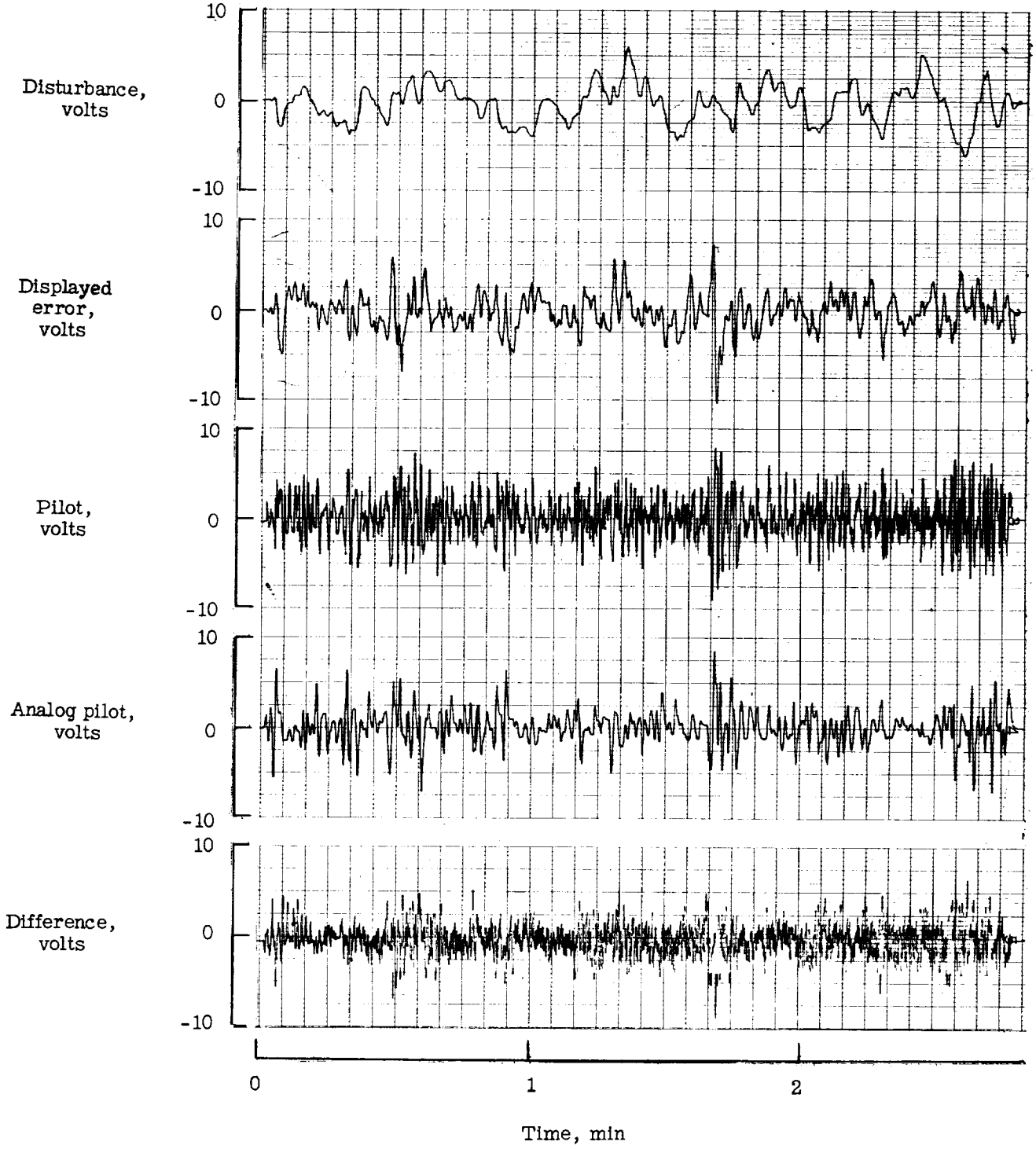

Figure 8.- Sample run with pilot E. Dynamics $\frac{10}{s^2}$.

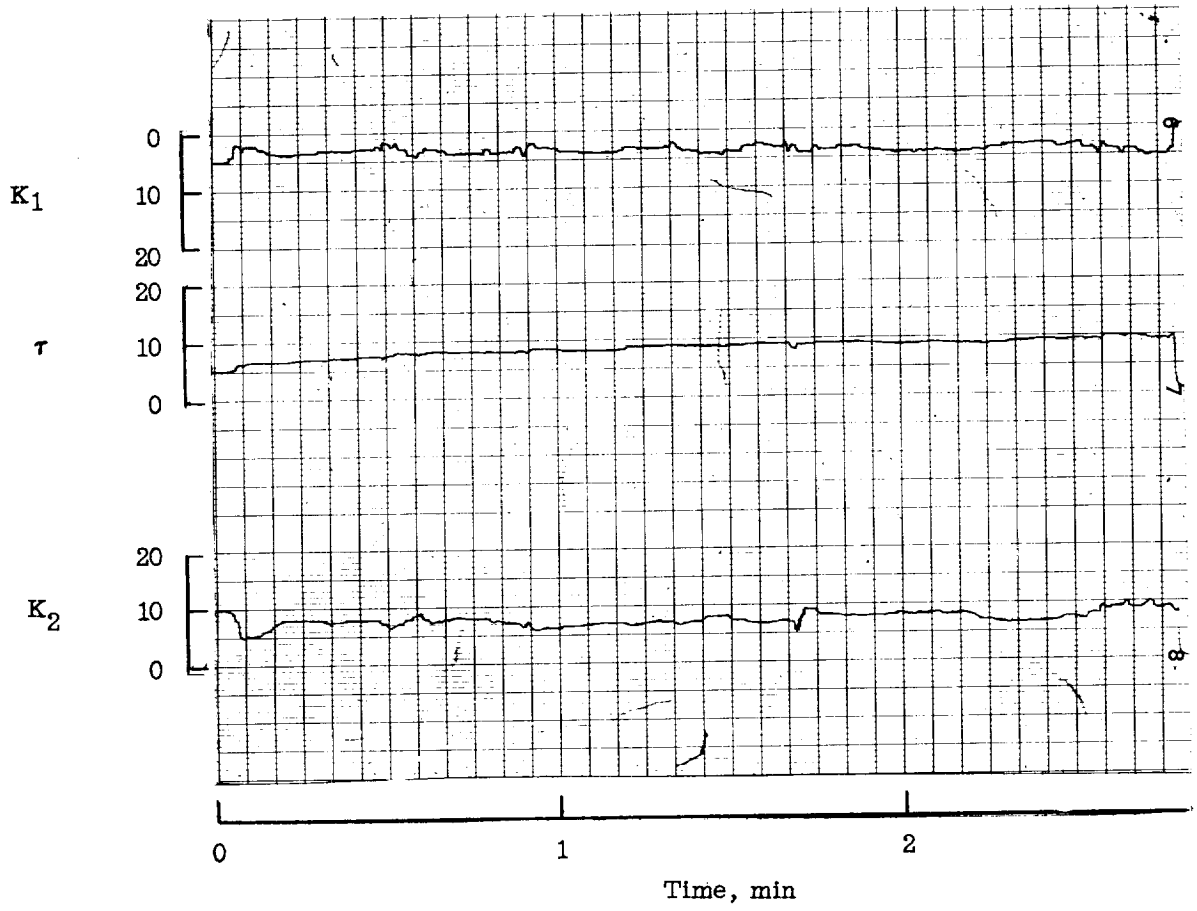

Figure 8.- Concluded.

Figure 9.- Sample run with pilot E. Dynamics $\frac{2}{s}$.

Figure 10.- Sample run with engineer G. Dynamics $\frac{10}{s^2}$.

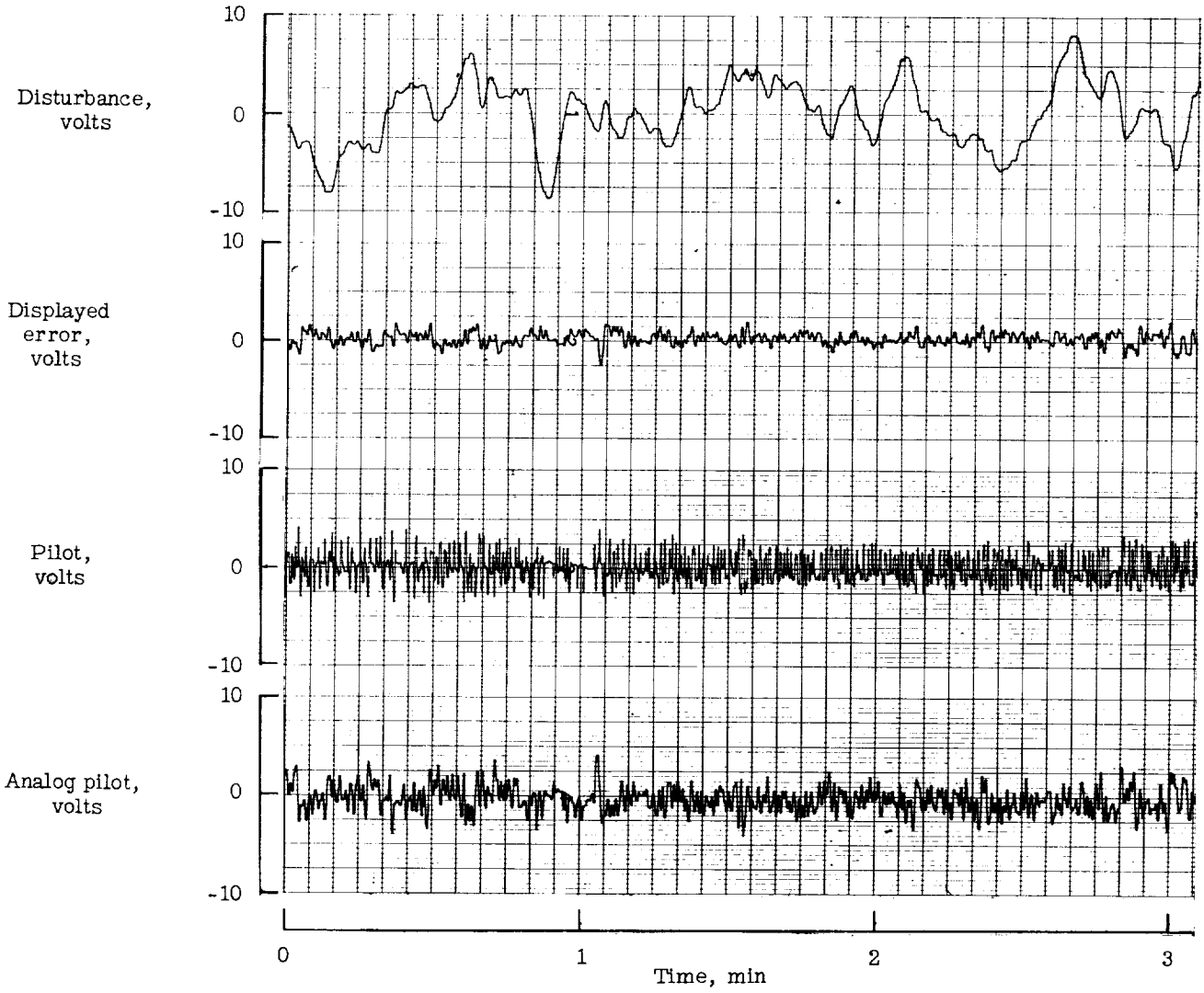

Figure 11.- Test with pilot A. Dynamics $\frac{10}{s(s + 1)}$.

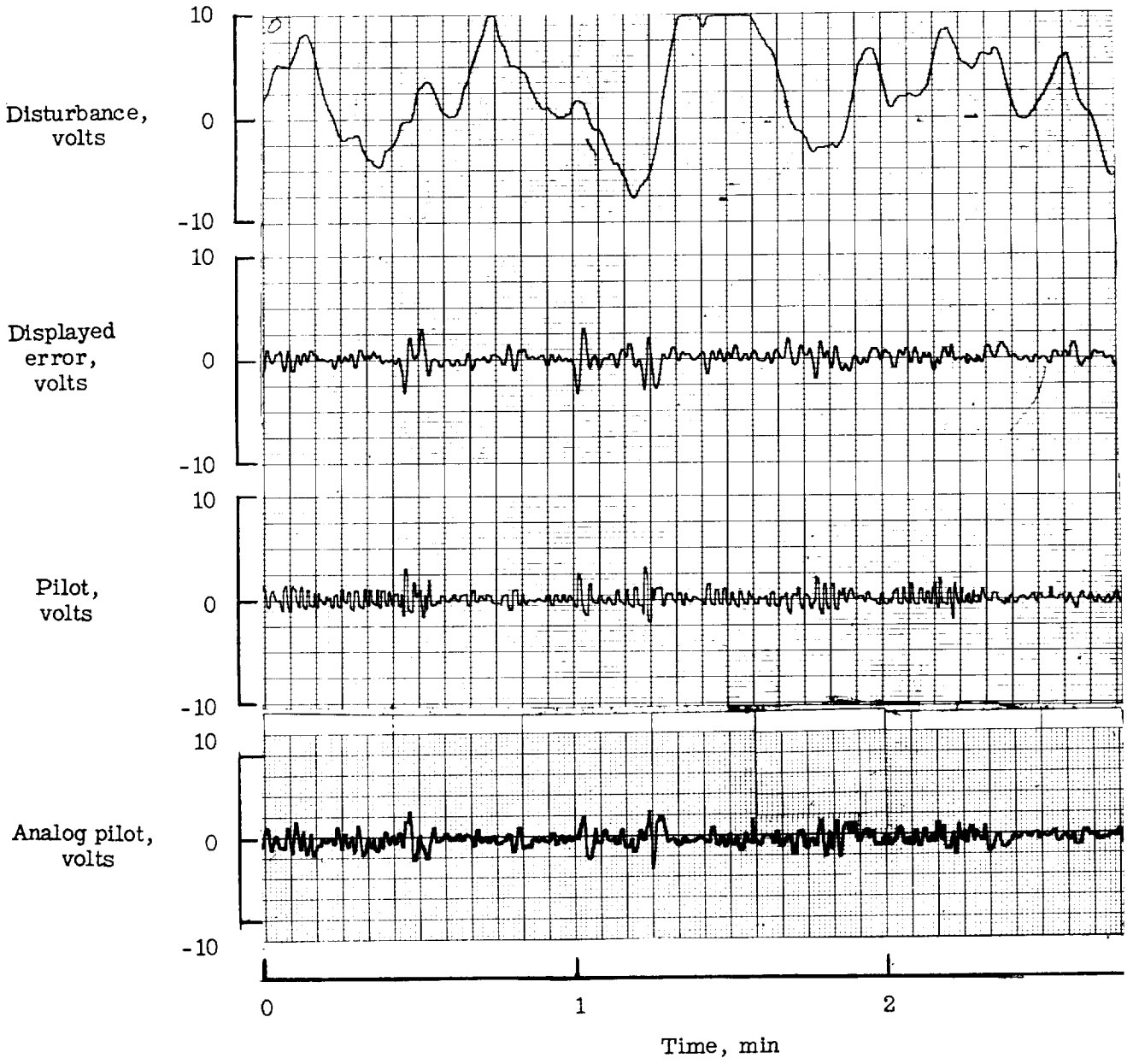

Figure 12.- Test with pilot B. Dynamics $\frac{10}{s(s + 1)}$.

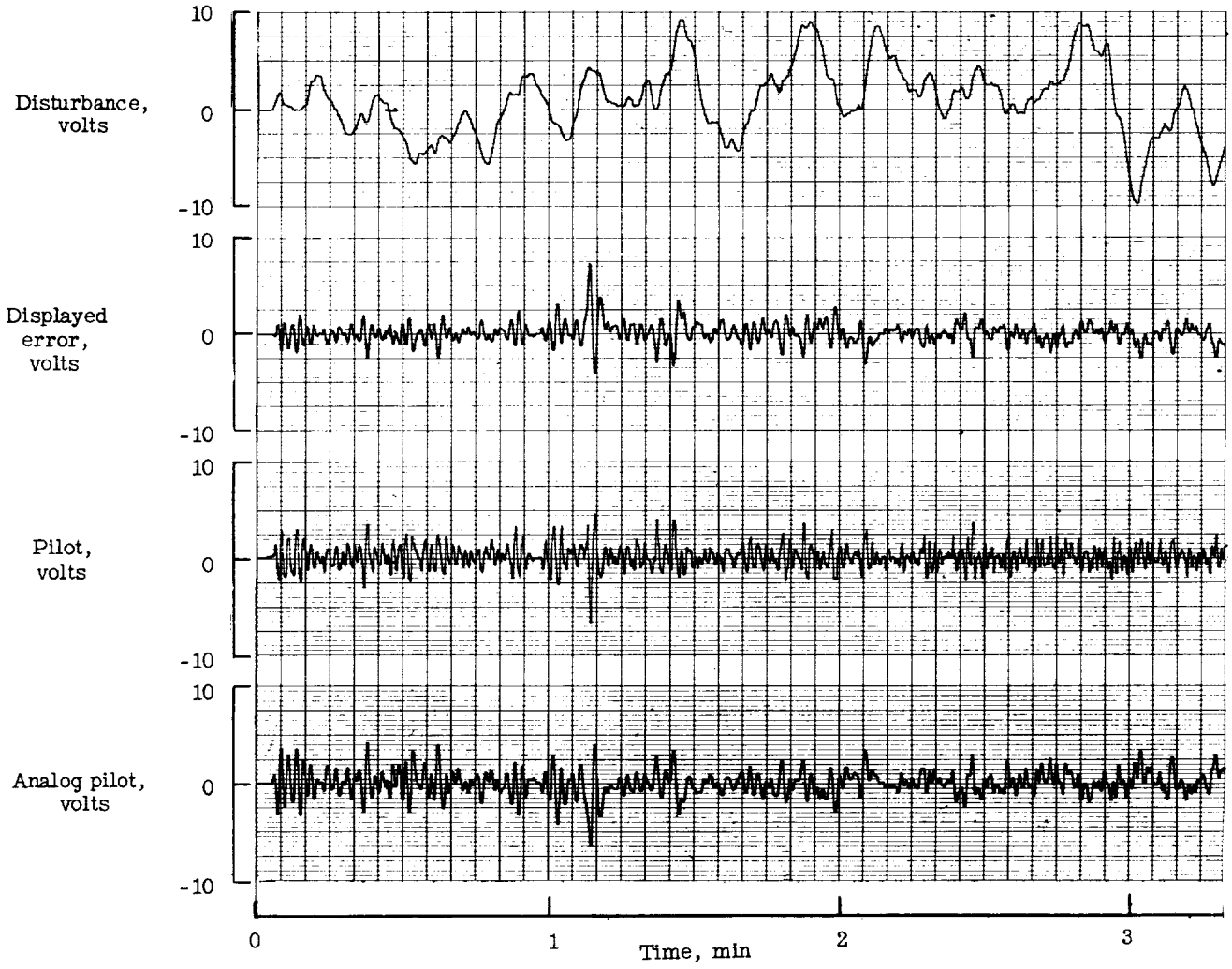

Figure 13.- Test with pilot C. Dynamics $\frac{10}{s(s + 1)}$.

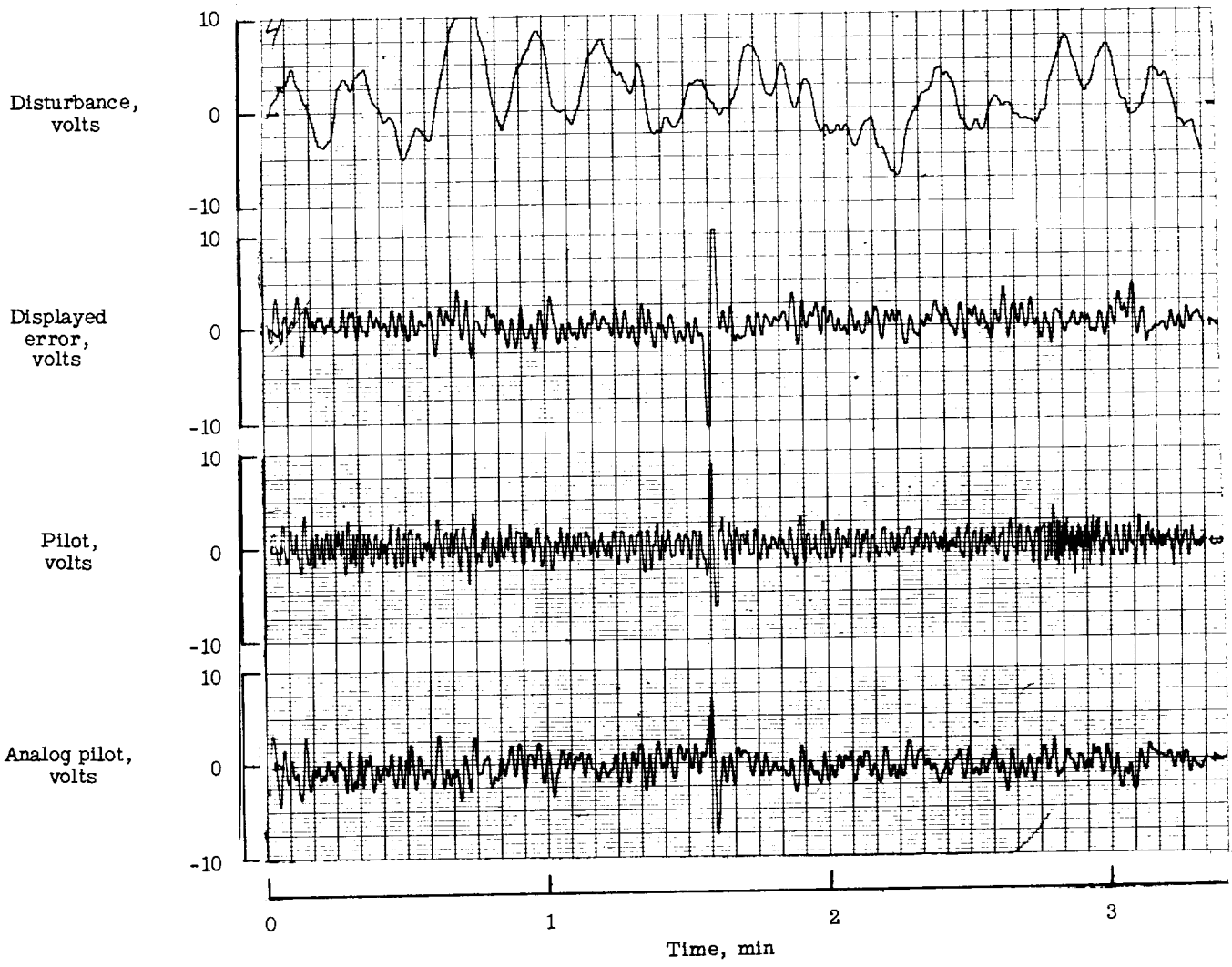

Figure 14.- Test with pilot D. Dynamics $\frac{10}{s(s + 1)}$.

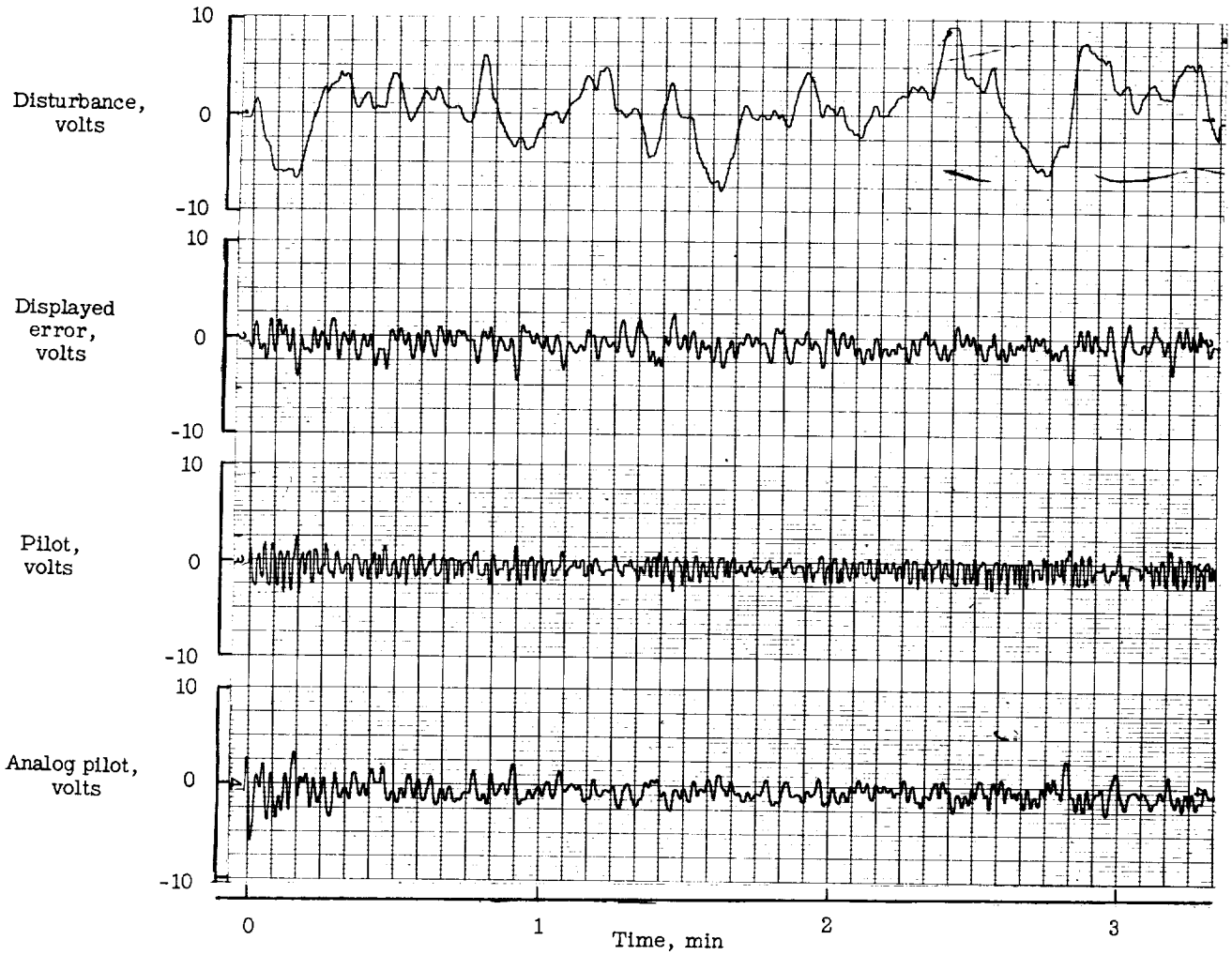

Figure 15.- Test with pilot E. Dynamics $\frac{10}{s(s + 1)}$.

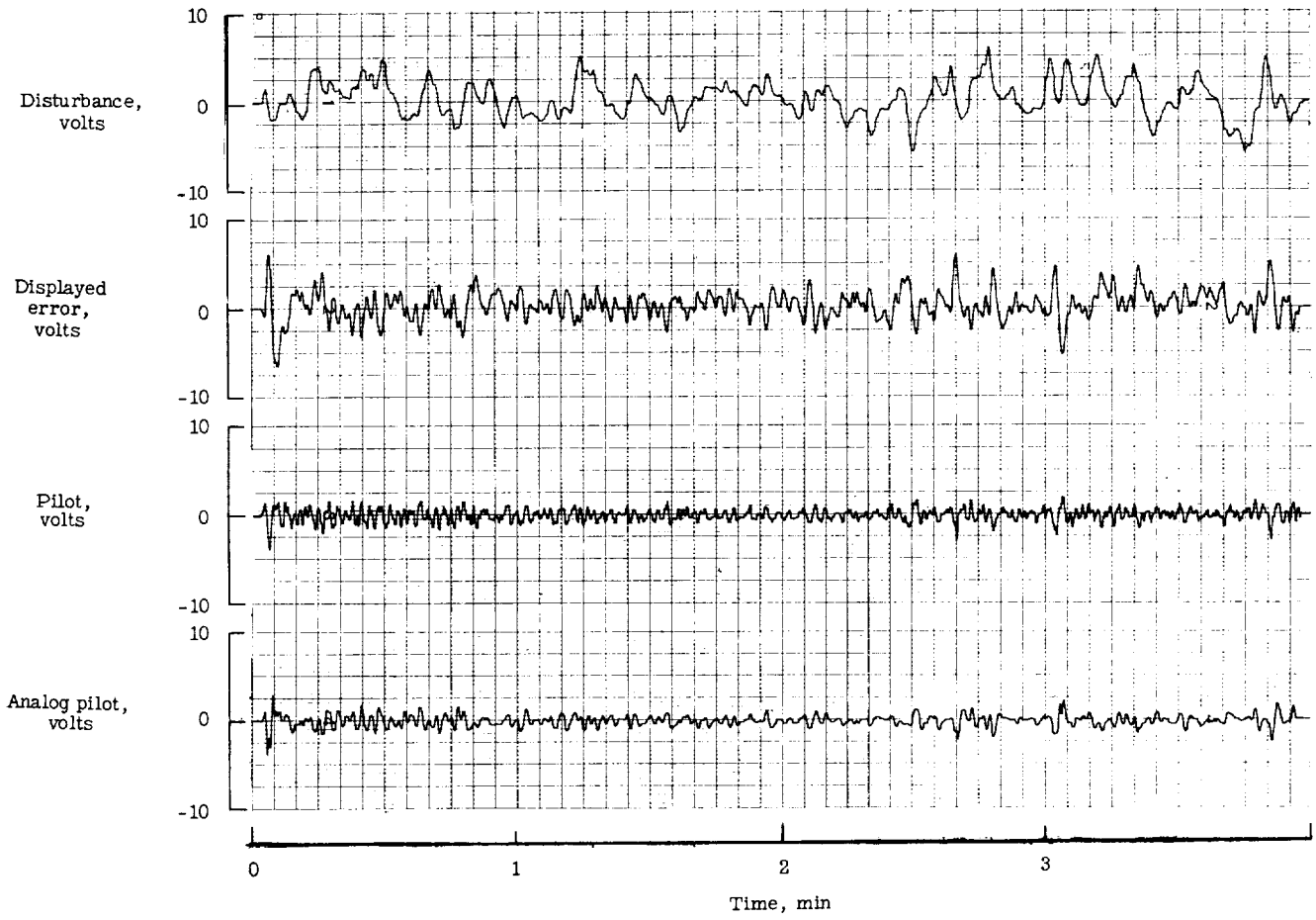

Figure 16.- Test with pilot F. Dynamics $\frac{10}{s(s + 1)}$.

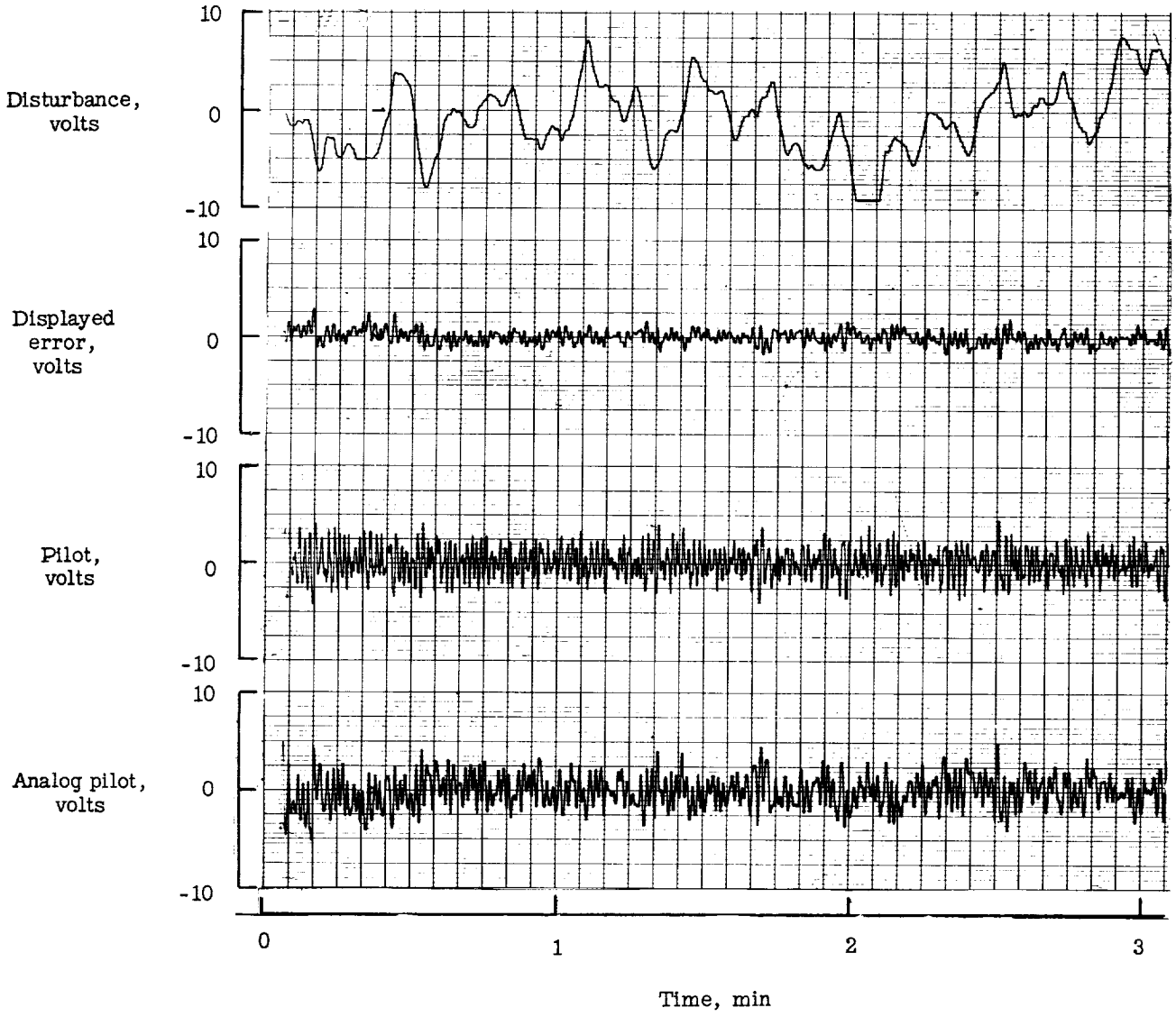

Figure 17.- Test with engineer G. Dynamics $\frac{10}{s(s + 1)}$.

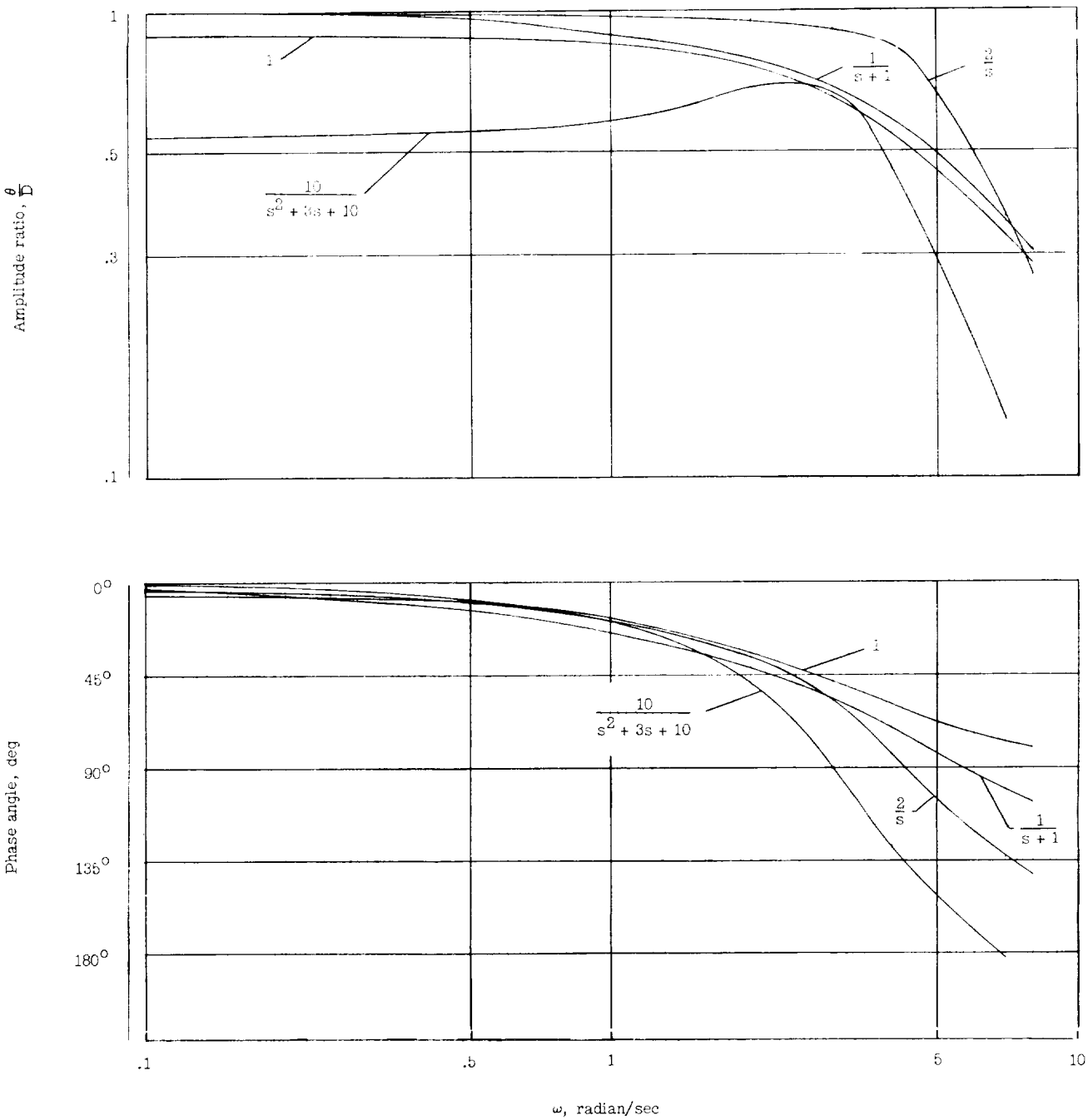

Figure 18.- Closed-loop frequency response with pilot E. (The curves are identified by the dynamics of the simulated closed-loop equations.)

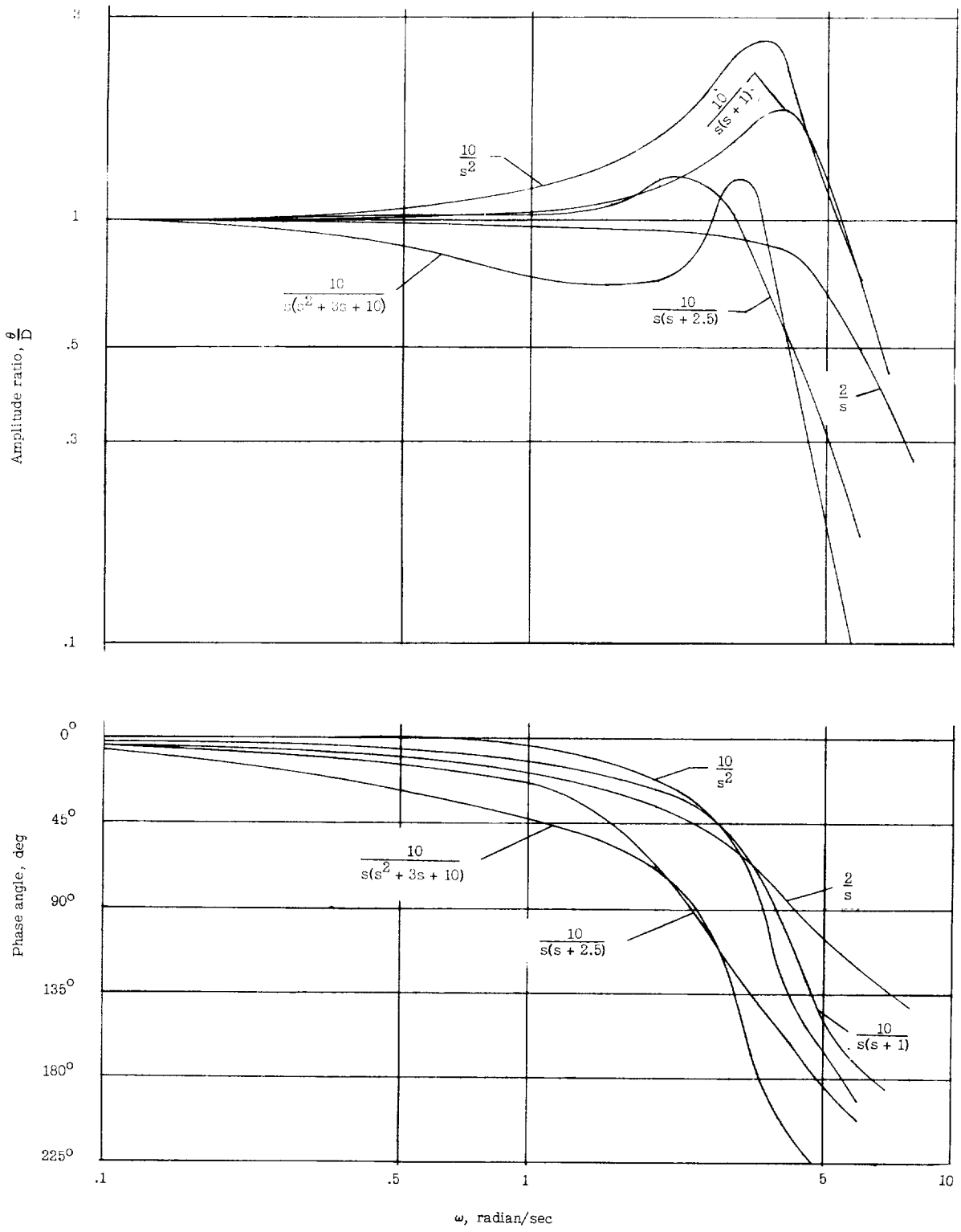

Figure 19.- Closed-loop frequency response with pilot E. (The curves are identified by the dynamics of the simulated closed-loop equations.)

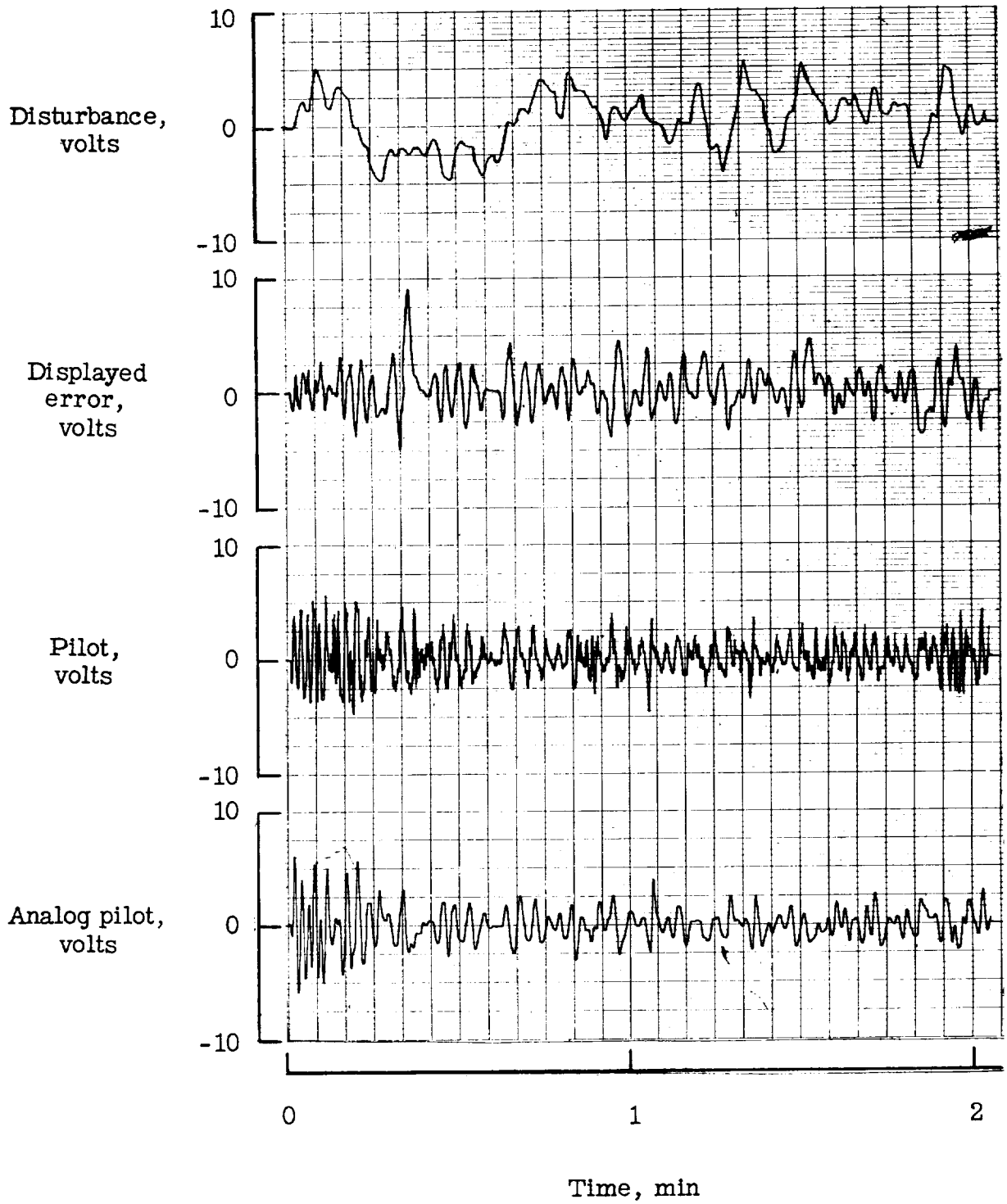

Figure 20.- Second-day test of pilot E. Dynamics $\frac{10}{s(s + 1)}$.

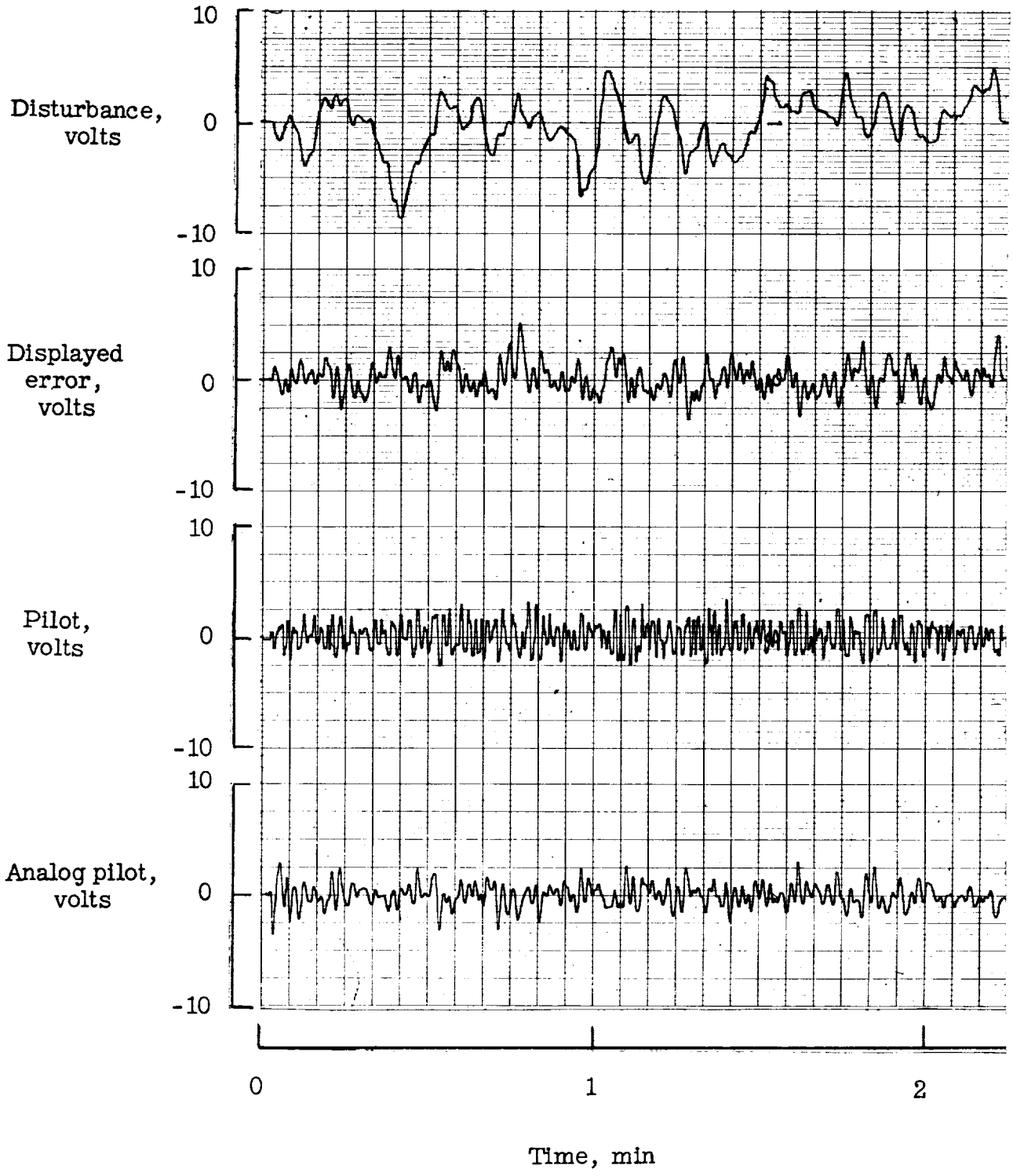

Figure 21.- Fourth-day test of pilot E. Dynamics $\frac{10}{s(s + 1)}$.

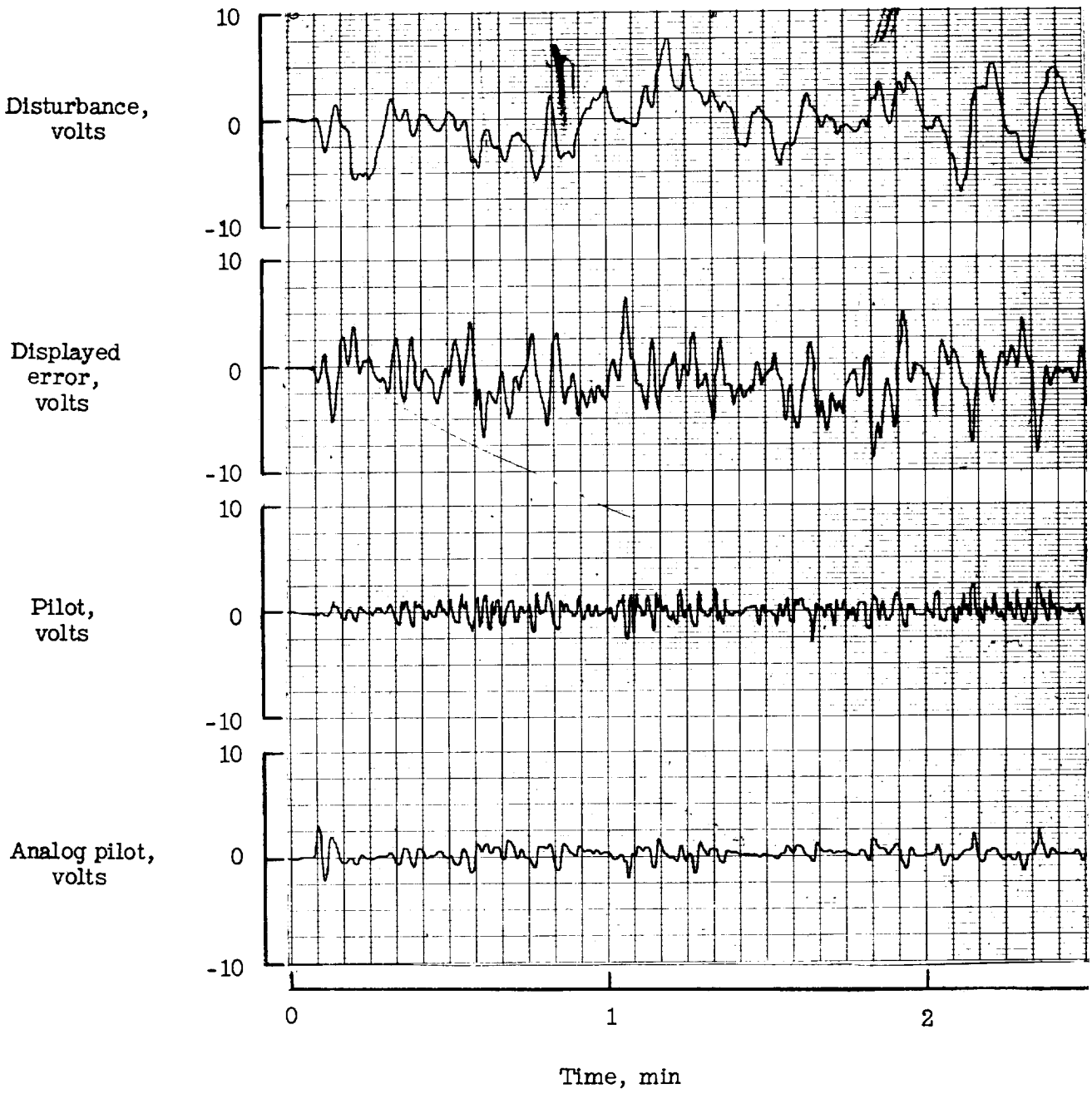

Figure 22.- Test with pilot E using insensitive display (50 volts/in.).

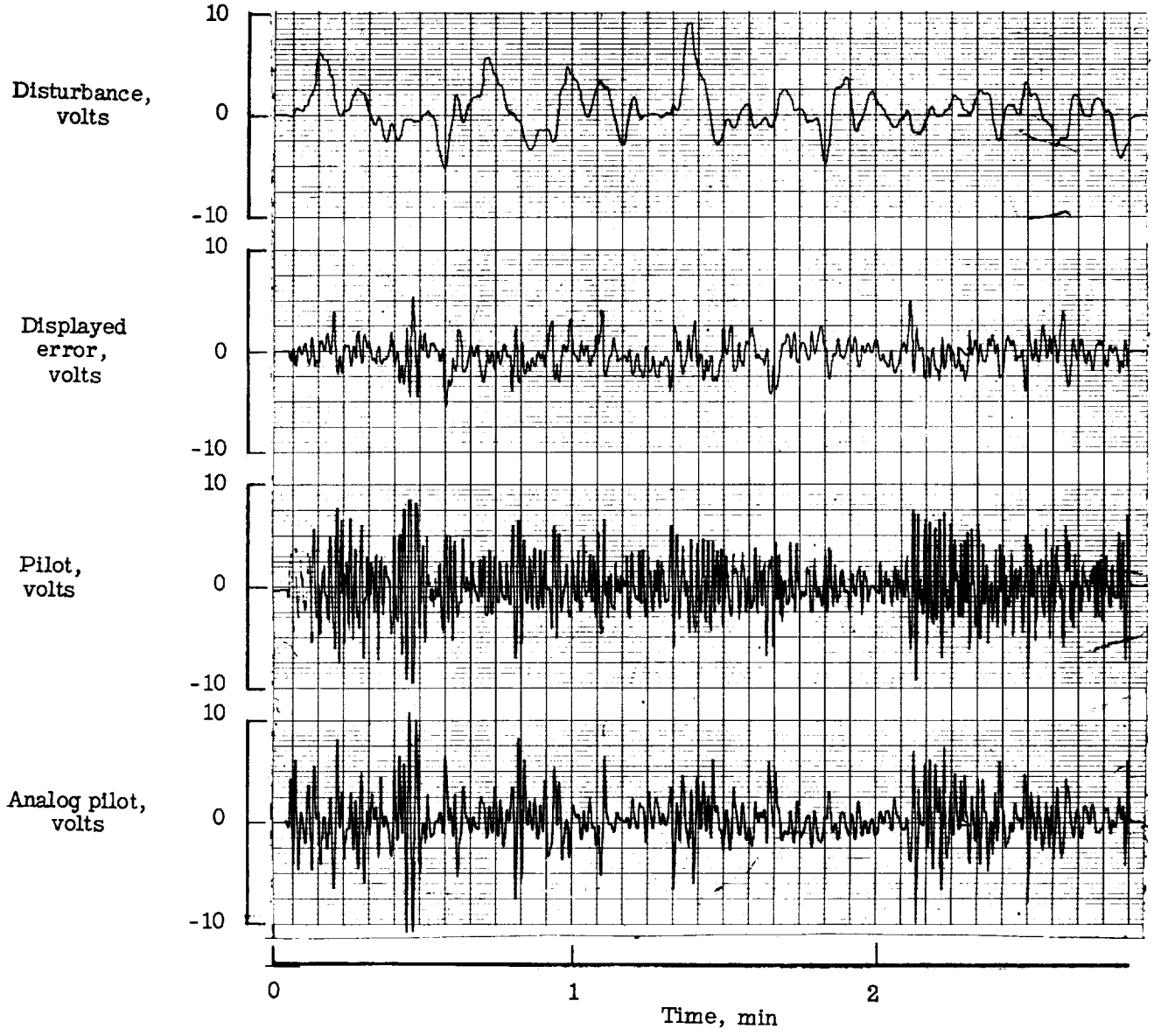

Figure 23.- Test with pilot E using sensitive display (1.25 volts/in.).

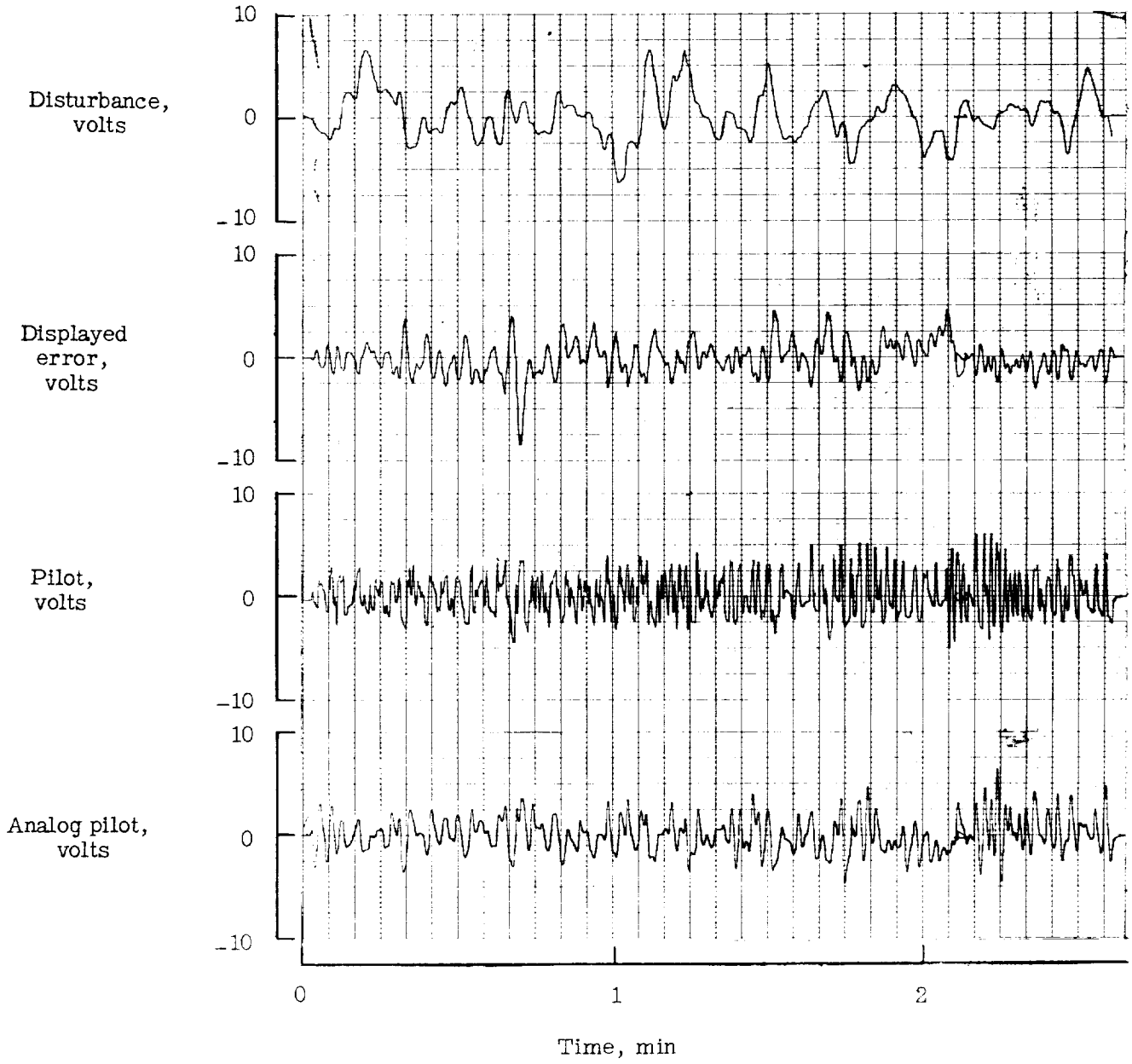

with pilot B using reduced control power. [illegible]

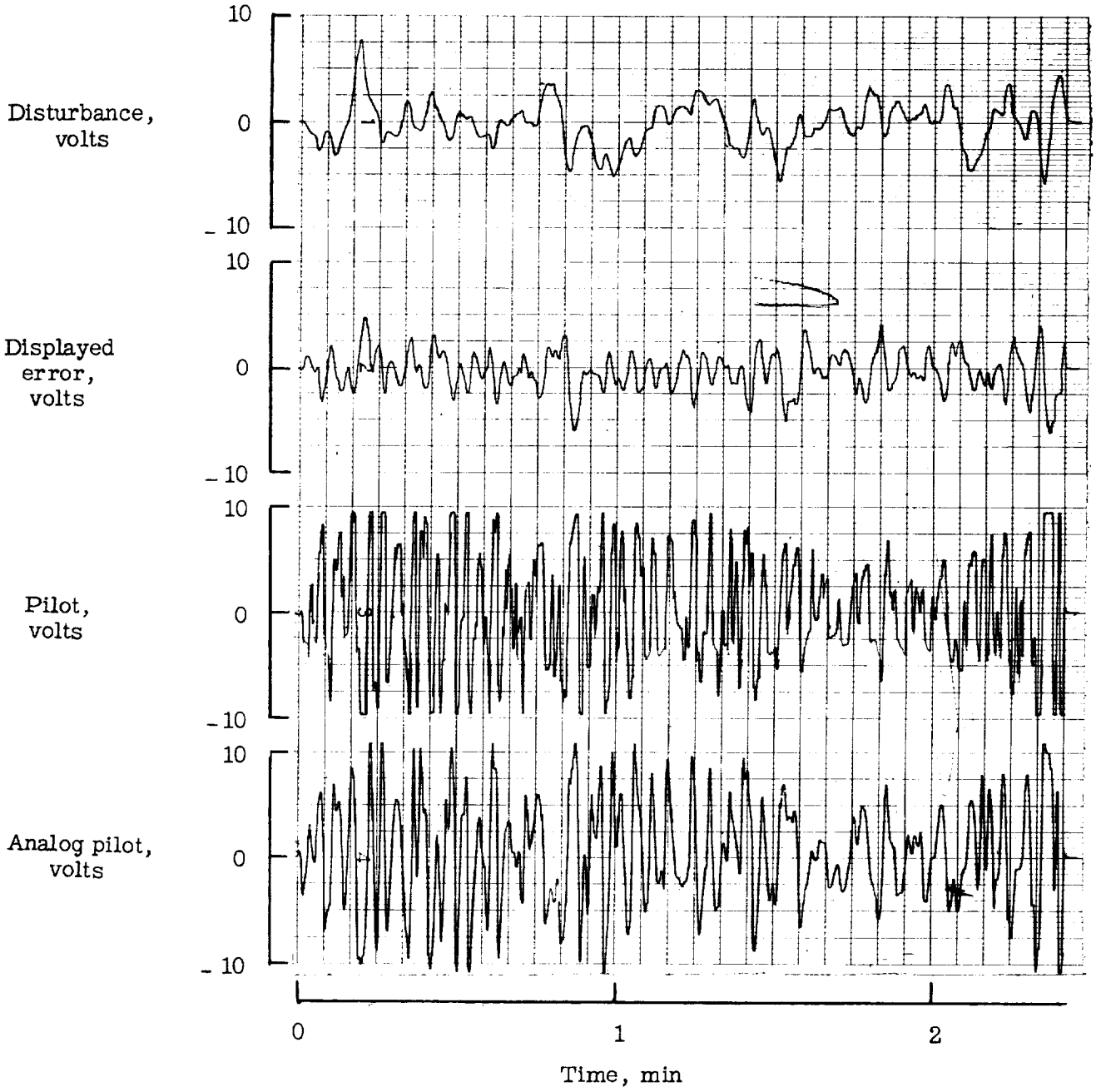

Figure 25.- Test with pilot E using low control power. Dynamics $\frac{1}{s(s+1)}$.

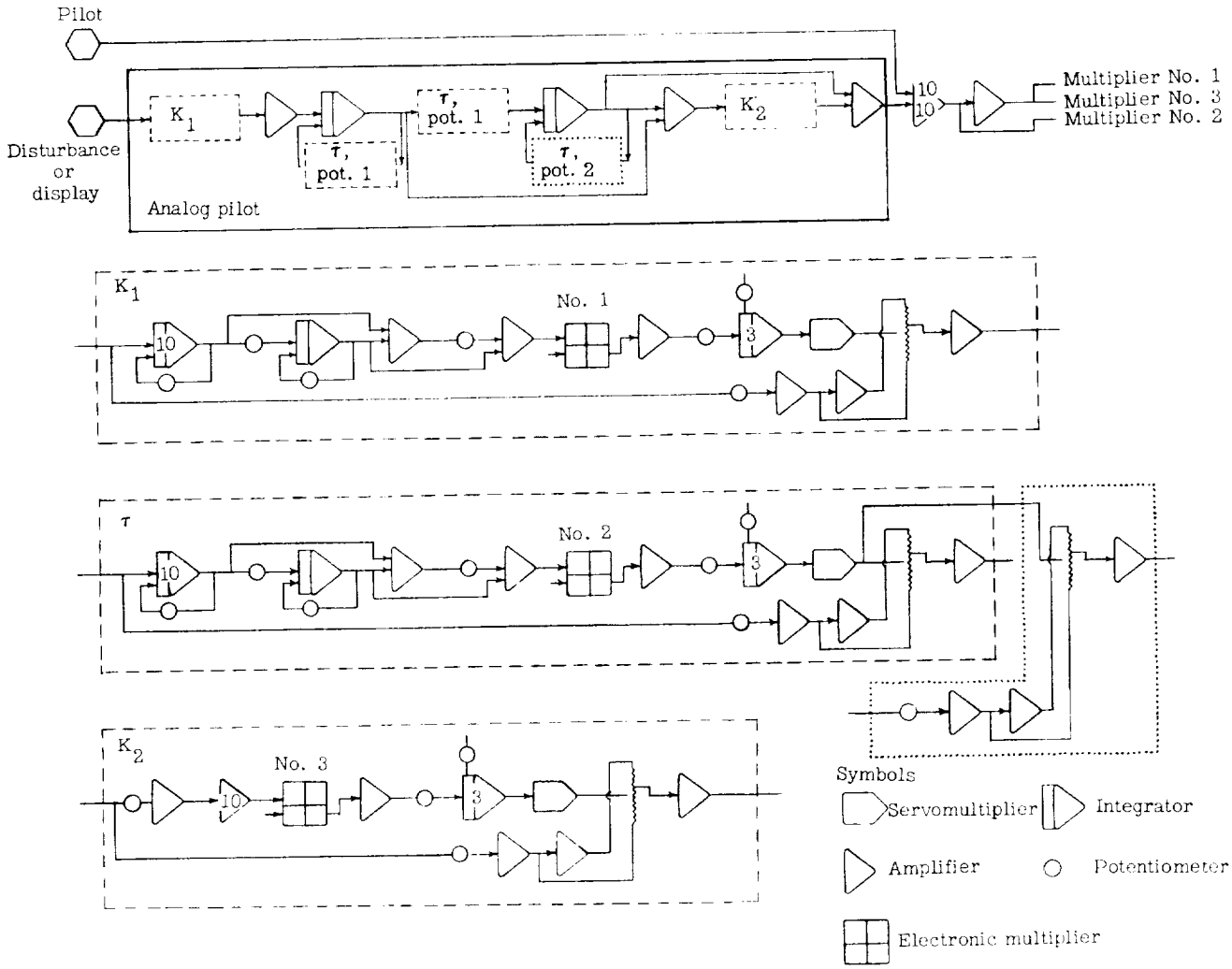

Figure 26.- Computer diagram of analog pilot and filters and servopotentiometers.

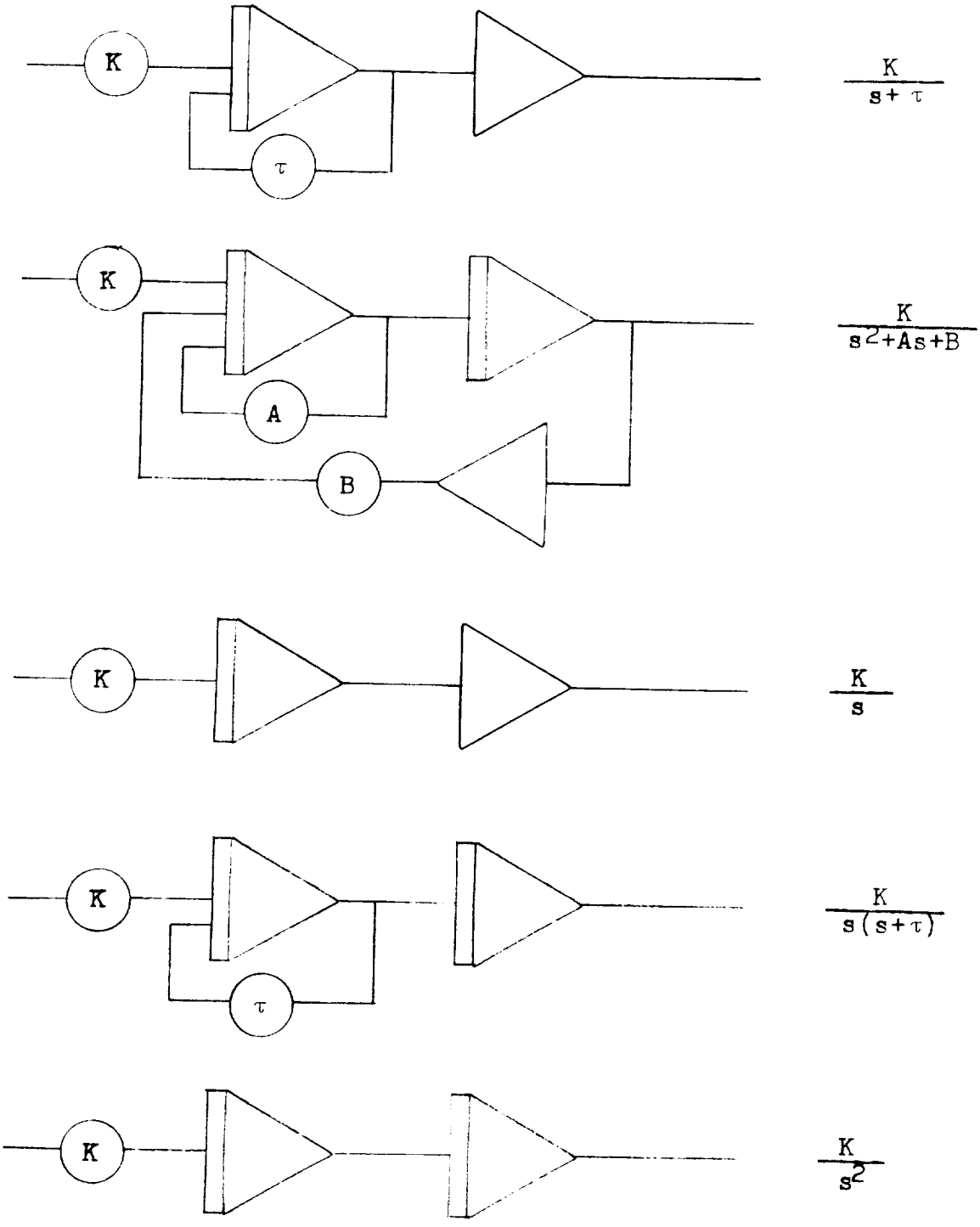

Figure 27.- Computer diagram of control dynamics.

NASA-Langley, 1963 L-3436